CORD-STEM CELL APPLICATION FOR REGENERATION ENHANCEMENT IN PORCINE MODEL

LIEW XUAN KAI JUSTIN
(B.Eng. (Hons.), NUS)

A THESIS SUBMITTED

FOR THE DEGREE OF MASTER OF SCIENCE
DEPARTMENT OF SURGERY
YONG LOO LIN SCHOOL OF MEDICINE
NATIONAL UNIVERISTY OF SINGAPORE

2016

DECLARATION

I hereby declare that this thesis is my original work and it has been written by me in its entirety. I have duly acknowledged all the sources of information which have been used in the thesis.

This thesis has also not been submitted for any degree in any university previously.

Liew Xuan Kai Justin
16 December 2016

Acknowledgement

The author would like to express his sincere appreciation and deepest gratitude to the following people for making this study possible.

A/Prof. Stephen Chang, for his supervision and funding support of the study. He has mentored the author beyond academic work and inspired the author towards completion of the project.

A/Prof. Phan Toan Thang, for his knowledge and laboratory skills. The author admires him for being an expert in his field.

Prof. Aileen Wee, for finding time despite her busy schedule to advice on the project's histological work.

Comparative Medicine Team, for their encouragement and friendship during animal studies. The author truly enjoyed his time working closely with them.

Neela Muthu, for her guidance and assistance in histological work.

Cecilia Chao, for her administrative support in making this thesis possible.

Xiaoyan, Donny and Francis, for being amazing colleagues who never stop supporting the author.

And, last but not least, Liew & Yeo family and Fiancée, for loving and caring the author. Without them, the author would not have been able to complete this project.

Table of Contents

Table of Tables

Table of Figures

Summary

Stem cells, known by their ability to repair damaged tissue, are often explored in regenerative therapies. The umbilical cord outer lining membrane was found to be a promising source of multi-potent stem cells. By cultivating the membrane in an epithelial cell growth medium, the cell population was found to possess the properties of both epithelial cells and embryonic stem cells. These cells were termed Cord Lining Epithelial Cells (CLEC).

Hepatocytes are epithelial cells and their proliferation upon liver injury is the main mechanism in restoring the liver. Earlier studies conducted showed that CLEC was able to be differentiated into functioning hepatocyte-like cells (HLC) and survive in immunologically competent specimens.

This study chooses porcine as a study model in developing CLEC as a treatment modality for liver failure. It aims to investigate the transplantation toxicity of HLC, unique cell delivery method and its enhancement effects on liver insufficient porcine models.

16 Yorkshire-Dutch Landrace pigs, with a mean weight of 40.5 kg were selected in this study. 50% hepatectomy was performed to simulate the liver insufficiency disease model. After the surgery, 4 pigs were transplanted with saline scaffold (control) while 7 pigs were transplanted with HLC scaffold (study). The remaining 5 pigs died on the surgical table and were left out from the study analysis.

The surviving pigs were studied for the subsequent 3 weeks. Liver function blood tests, computed tomography (CT) scans, CT-guided needle biopsy at

selected intervals were performed. At the end of 3 weeks, all subjects were sacrificed unless advised by the veterinarians for earlier termination. Liver volumetric data was collected throughout the 3-week survival period. The excised liver and biopsy tissue samples were examined histologically.

DeRitis ratio, blood prothrombin clotting time, serum alkaline phosphatase and liver volume data showed no statistically significant difference between the two groups. One subject from the control group and the study group were euthanized before the end of post-operative 3 weeks due to intestinal adhesion. Liver biopsy samples showed minimal and non-specific reactions in both groups. Histology study showed the collagen scaffold were absorbed by the host within 3 weeks. No signs of significant cellular rejection were observed along the transplant interfaces. Immunohistochemistry staining showed HLC survived within immunologically-competent pigs for 3 weeks after transplantation.

From this study, the group concluded that HLC poses insignificant toxicity in a xeno-transplantation model as no significant difference were observed between the study and control group. No immune-rejection response was elicited in the study subjects. The unique cell delivery method transported HLC to the host with 3 weeks' survival but cells were attached to the scaffold surface superficially. While a positive trend was developing, HLC did not show significant effect in accelerating liver regeneration nor increasing liver function throughout the 3 weeks' post-transplantation in this study.

Introduction

Liver disease is a huge burden to public health globally. In 2010, mortality due to liver diseases accounted for over 2 million deaths, approximately 4% of all deaths in the world [1]. As the patient's liver degenerates, transplantation of another liver, either from a deceased person or a living donor, is often the only available curative treatment. According to the 2012 Scientific Registry of Transplant Recipients, there were 10,000 new candidates added to the United States liver transplant waiting list, but only about 6,000 liver transplantations were performed that year [2]. With a shortage of liver donors, alternate forms of treatment therapy are heavily investigated to meet the demands of increasing liver failure incidence rates worldwide.

Our research aims to use hepatocyte-like cells (HLC) derived from Human Cord Lining Epithelial Cells (CLEC) as a mean to enhance liver regeneration, before the liver worsens to a stage in which regeneration is not possible, such as the formation of regenerative nodules. Patients suffering from acute liver failure due to drugs or post-surgery and patients suffering from chronic liver disorders stand to benefit the most from accelerated liver regeneration. This initial study aims to investigate the safety of implanted HLC in the recovery of pigs that have undergone extensive hepatectomy and the effectiveness of the unique delivery method.

Objectives

The main objectives of this project were as listed:

1. To evaluate the toxicity of HLC in a xeno-transplanted model:

   a. Viability of HLC and signs of cellular rejection along transplant interface in hosts after 3 weeks were investigated
   b. Overall health of subjects over the period of 3 weeks after transplantation of HLC were observed

2. To evaluate the effectiveness of novel cell delivery method – placing collagen scaffold directly on resected liver surface:
   a. Histological study of collagen scaffold, before and after transplantation were carried out
3. To investigate the effectiveness of HLC in enhancing liver regeneration on liver insufficient porcine models:
   a. Liver function tests (LFT) and liver volumetric study were carried out over the period of 3 weeks after transplantation of HLC

Scope

In this project, the team aimed to evaluate the toxicity and effects of HLC as the first step in developing CLEC as a treatment modality for liver failure. 16 adult pigs were chosen for this study and 50% hepatectomy was performed to create a liver insufficient animal model. After the surgery, the subjects will either receive a saline soaked collagen scaffold (control) or HLC soaked collagen scaffold (study) and were monitored periodically. At the end of 3 weeks, all subjects were sacrificed unless advised by the veterinarians for earlier termination.

The respective investigations were carried out as highlighted in the objectives of this study and data was collected. Analysis of data, image processing as well as consultations with clinical experts were performed and reported in this report.

Literature Review

Liver Cytology

The liver is the largest internal human organ and an average adult liver weights about 1,400 g. Based on external anatomical structure, the human liver can be divided into 4 lobes: Left, Right, Quadrate and Caudate respectively. French surgeon Couinaud proposed further segmenting the human liver into 8 portal territories based on its internal architecture [3]. Each segment has its own arterial supply, venous and biliary drainage, number in a clockwise manner, shown in Fig. The human liver is highly vascular and has a unique dual blood supply (about 1600 mL/min), up to 80% comes from the portal vein and the rest from the hepatic artery. 10-15% of the total body blood volume remains in the liver, an extremely high proportion compared to other internal organs [4, 5].

Porcine models are commonly used in experimental surgery due to their resemblances with the human morphology and size. Like the human liver, pig's liver can be described as having 4 lobes and further divided into 8 surgical segments. The segmental nature of the pig liver acts as a good template for the investigation of liver surgery, transplantation and hepatic regeneration [6].

Liver physiology between the humans and pigs are highly similar too, owing to their respective microarchitectures. Hepatic lobules, the functional units of liver, were first described in pigs in 1664 (see Figure 1). In the human liver, these microscopic unit amount to over a million count and are approximately 1mm wide. Hepatic lobules are primarily made up of the portal fields, hepatocytes sheets, sinusoids and the central veins (see Figure 2).

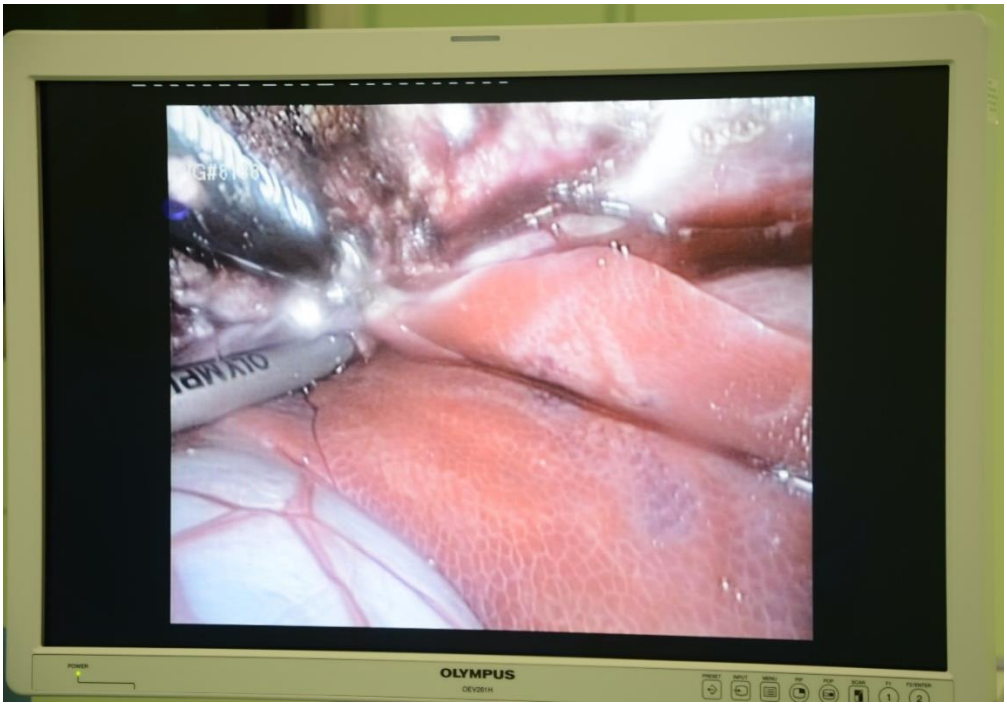

Figure 1: Hepatic lobules on porcine liver surface. The porcine's hepatic lobule is outlined by the connective tissue septum, allowing different lobules to be clearly visible on the laproscopy monitor. Image is taken during the hepatectomy procedure of ADD2 subject.

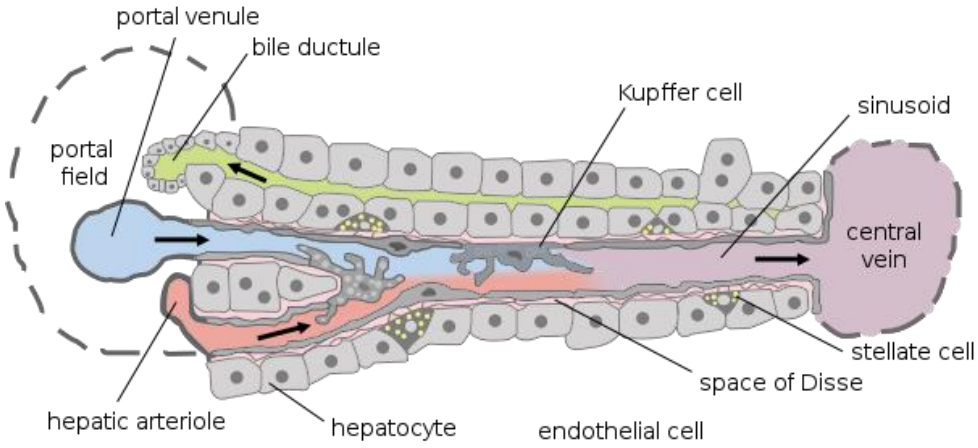

Figure 2: Structure of the mammalian hepatic lobule. Left-to-right arrows show the flow of blood through the sinusoid while right-to-left arrow show the draining of bile through the portal field. Image adapted from [7].

The portal field contains the triad of tiny branches of the portal vein, hepatic artery and bile ductile, together with nerves and lymphatic vessels. The triad travel together within portal fields of adjacent lobules. The portal vein and hepatic artery deliver oxygenated blood with nutrients into the sinusoids. The

exchange between the hepatocytes and surrounding blood sinusoids enables many metabolic processes to take place. Hepatocytes are polygonal epithelial cells and they are arranged in 2-D unicellular plates. These plates overlap and form complicated 3-D walls, seen in the lobules. Consequently, blood with detoxified substances and metabolic end products flows out of the sinusoids, into the central vein. The central vein ultimately reunites with the hepatic vein transporting these substances out of the liver. On the other hand, bile generated by hepatocytes travels in the opposite direction through bile canaliculi and drains into the bile ductules of the triad [4, 8].

The liver lobule can be defined according to multiple perspectives and has constantly evolved over time as more findings are reported (see Figure 3). The classic hepatic lobule or central vein lobule, based on the structural appearance, resembles a hexagon with portal fields at the corners and the central vein is located in the center of the lobule. Blood flows in a centripetal direction while bile flows centrifugally towards the periphery. The portal vein lobule is based on the bile-formation characteristic of the liver. The portal field is located at the center while the central veins form the limiting points of the lobule. Blood flows from the center towards the periphery while bile flow in the opposite direction, produced in the surrounding hepatocyte plates.

Recent findings show that hepatocytes are structurally heterogeneous based on their positions with respect to the portal vein. This leads to the more recent hepatic acinus model which takes into account the “zoning” nature of the hepatocytes. Zone 1 is the periportal region, closet to the portal vein lobule while Zone 3 is the perivenous region, closet to the central vein. Ultra-cellular structures in the hepatocytes also varies in different zones. Mitochondria and

the Golgi structures are more numerous in Zone 1 than in Zone 3. On the other hand, there is less smooth endoplasmic reticulum in Zone 1 compared to Zone 3. Furthermore, cellular multiplication was shown to take place in the periportal region and subsequently migrates to the center, suggesting that hepatocytes are highly pluripotent cells.

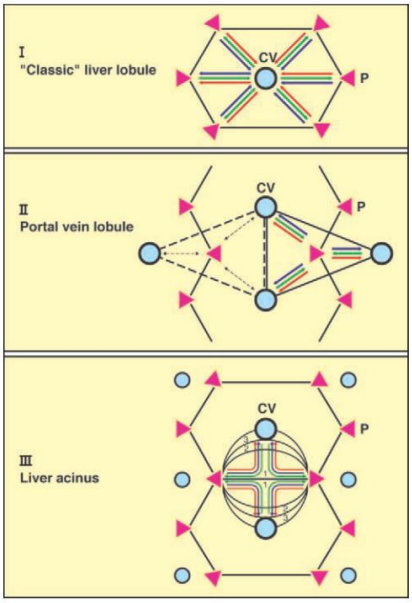

Figure 3: Different views on the basic unit of the liver. CV represents central vein, P represents portal field, blue arrow represents venous blood flow, red arrow represents arterial blood flow and green arrow represents bile flow. Image taken from [4].

Despite its simple architecture, the liver performs numerous vital biochemical processes, such as metabolism of oxidative energy, xenobiotics and bile formation, either continuously or in biological rhythms. To maintain homeostasis in the body, an intricate level of control is required. The zonation of the hepatic acinus model demonstrates how two physiologically opposite metabolic processes, gluconeogenesis and glycolysis, could be performed simultaneously by hepatocytes in the periportal and perivenous regions respectively. Various metabolic pathways are compartmentalized to specific regions along the hepatocyte plate and allows for differential expression of

proteins across zones. The liver produces most of the circulating proteins, including the main blood plasma protein, albumin. The human liver synthesizes 200mg of albumin per kg of body weight per day. [9, 10]

Laboratory Diagnostics

Being a critical organ of the body, it is clinically necessary to monitor and being a critical organ of the body, it is clinically necessary to monitor and quantify the functioning of the liver. Hepatocellular damage is typically assessed by measuring enzymes that were released into the blood through the damaged plasma membranes of the hepatocytes. The most frequently used indices are serum concentrations of aspartate aminotransferase (AST) and alanine aminotransferase (ALT). These enzymes, which are involved in the pathways of gluconeogenesis, catalyse the enzymatic transfer of the α-amino group from the respective amino acid, aspartate or alanine, to α-ketoglutarate, yielding glutamate and, respectively, oxaloacetate or pyruvate. The enzyme levels are commonly determined in laboratories via spectrophotometry of the formation of NAD+, which correlates directly with the concentration of aminotransferase of the sample [11, 12].

Aminotransferases in serum are usually elevated during hepatocellular injury of any cause and ALT value generally exceeds AST value due to the location of the different enzymes. ALT is localized exclusively in the cytosol of hepatocytes while majority of AST is found in the mitochondrial membrane. Only during cellular necrosis with associated destruction of mitochondria does the AST value exceeds that of ALT. Hence, this constitutes the basis for the

DeRitis ratio (AST/ALT). It was suggested that a DeRitis ratio above 0.6 is associated with a poor outcome in cases of severe acute hepatitis while a ratio above >2 is indicative of alcoholic or malignant liver diseases.

Lactate dehydrogenase (LDH) is another marker for hepatocellular damage. LDH is a cytoplasmic enzyme which catalyzes the reversible conversion of lactate to pyruvate, utilizing NAD+/NADH as a cofactor. It exists as five different isoenzymes and is found in almost all tissues in varying concentrations. Increased release of LDH from damaged, dying or metabolically deranged cells in any of these tissues may cause an elevated serum LDH concentration. Specifically, for the liver, marked elevation of serum LDH is indicative of liver metastases and obstructive jaundice. It is commonly measured using photometric assessment of the oxidation rate with NADH.

The synthetic ability of the liver can also be assessed from certain plasma protein concentrations, such as albumin (ALB), produced selectively by the liver. ALB is a single, un-glycosylated polypeptide chain of 575 amino acids (molecular mass 69 kDa). It is synthesized exclusively by hepatocytes and has two principal functions in plasma: maintenance of osmotic pressure and transport of compounds through reversible binding. Binding with dyes, such as bromocresol green or bromocresol purple, in pH 4.15 is often used in laboratories to detect the concentrations of serum albumin. Due to its long half-life (14 – 21 days), severe acute liver diseases only exhibit decreased ALB concentration during the later course.

Another common synthetic assessment used is prothrombin time (PT). This test reflects the functional presence of factors involved in the blood clotting pathway, which are produced specifically by the liver. Sodium citrate is often used as anticoagulant and comes as premix in the blood sample collection tube. The result (in seconds) is determined from the time of the addition of calcium and tissue thromboplastin to the time of the clot formation. An extended time to clot formation is suggestive of impaired hepatocyte synthetic function. The International Normalized Ratio (INR) was devised to standardize PT results between manufacturers, due to variations in the type of factors used in performing the test.

Weakening of the excretory functions of the liver can be indirectly assessed from increases in the plasma levels of compounds that are normally cleared by the liver and secreted in bile. Bilirubin, a yellow pigment, is an example of such compounds. A product from the breakdown of aged red blood cells, it exists in the body as either unconjugated or conjugated forms. Unconjugated bilirubin (IB) is insoluble in water and majority is found in serum. Hepatocytes uptake unconjugated bilirubin from the blood circulation and is where conjugation with glucuronic acid takes place. This renders the conjugated bilirubin (DB) water-soluble and is secreted together with bile into the intestines and finally expelled with faeces.

Spectrophotometric method is commonly used in laboratories to measure the concentration of serum bilirubin. Bilirubin reacts with diaotized sulfanilic acid to produce azo pigments. ‘Accelerator’ compounds, such as caffeine or ethanol, are added to hasten the reaction of IB, to produce the result of total bilirubin

concentration (TBIL). In a healthy person, none or low concentrations of conjugated bilirubin is found in the serum as they are removed via the biliary pathway. Conjugated hyper-bilirubinaemia is indicative of significant hepato-biliary disease. On the other hand, unconjugated hyper-bilirubinaemia could suggest shunting around the liver of portal blood.

Alkaline phosphatase (ALP) is a metabolic enzyme located in the cells, lining the biliary ducts of the liver. Elevated level of ALP is highly indicative of biliary obstruction or bile secretion dysfunction. The increase secretion of ALP into blood is stimulated by bile acids. ALP activity is assayed enzymatically, utilizing the hydrolysis of phosphate esters.

There is no single biochemical method which provides a global statement on the hepatic function itself. It is often that these assessments are carried out and examined together to reveal typical patterns of different pathophysiological conditions, as well as the severity of the liver disease. Hence, health institutions utilize a series of mentioned assessments, known as hepatic panel or LFT to evaluate the patient's liver condition. Shown in Figure 4 is a result slip of National University Hospital's Liver Panel.

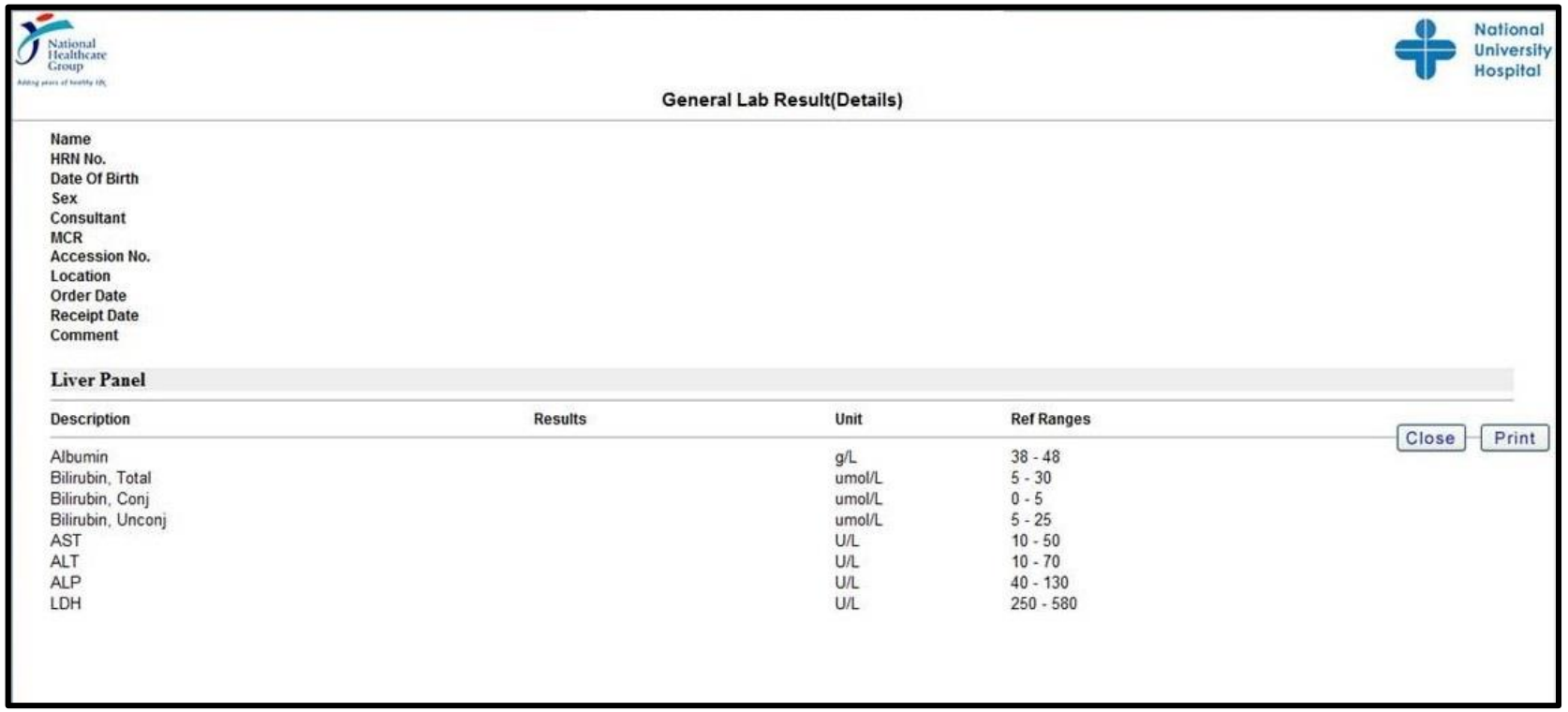

Figure 4: Overview of general liver panel test. Image taken from National University Hospital.

Imaging and Histology of Liver

Imaging the liver is just as important as its laboratory diagnostics. A computed tomography (CT) scan is a common imaging method to create pictures of cross-sections of the liver. CT scan uses the attenuations of many finely focused X-rays, which are subsequently measured by multiple detectors and converted to electrical signals. These values are then transmitted to a computer to calculate the absorption value of each image point and relaying it into a complex digital image. A sequence of arterial, portal-venous and delayed phase imaging has been developed to display and differentiate between the hepatic arteries, portal and hepatic veins, and the hepatic parenchyma. This is known as the triple phase liver CT. Contrast agent, such as Omnipaque (iohexol), is introduced into the patient's body rapidly via intravenous injection. The liver is subsequently scanned at specific time intervals to achieve the required multiphase images [13].

A group from I^2R had recently developed a system to measure the liver volume through CT images. From the collected CT images, a rough 3D liver volume was automatically segmented using 3D mesh deformation-based method. A refinement step was subsequently introduced to eliminate the segmentation error by using a 3D post-editing tool, followed by mesh-volume conversion to determine the liver volume. According to a study by Nieheus et al., high correlation was discovered between CT-based and water displacement methods to measure liver volume. CT-based volumetric method was found to be 13% higher than water displacement volumetric measure. (p <0.0001). The factor leading to the difference between *in-vivo* CT volumetry and *ex-vivo* water

displacement methods was due to blood perfusion of the liver *in-vivo*. It was recommended that a systematic difference of 13% has to be taken in account when dealing with these two methods [14-16].

The microscopic analysis of cells and tissue play in important role in today's clinical diagnosis, commonly known as the field of Histology. The process of a typical histological assessment begins with the collection of tissue specimens. This can be done via biopsies, large organ resections or from cytological examinations. This is followed by tissue fixation for two purposes, to delay the decay process and to preserve the cellular architecture and composition for downstream analysis. Specimens are immersed in specific groups of chemicals, known as fixatives, for this purpose. Formalin is the most commonly used fixative due to its low cost and high degree of adaptability. Used in this study was 10% neutral buffered formalin, consisting of 3.7% formaldehyde in water and monosodium phosphate salts. Formaldehyde, in aqueous solution, forms methylene glycol. When specimens are immersed in formalin, they are rapidly penetrated by methylene glycol. Within the tissue, formaldehyde dissociates and cross-links with the various functional groups of biological macromolecules. The initial cross linking is completed within 48 hours after penetration and forms stable covalent cross linkages over time. It is known in the field, prolonged storage of specimens in formalin yield poor antigen and gives rise to false negative results.

Tissue processing is recommended after 2 days of tissue fixation. Fixed tissue is dehydrated with alcohol and xylene and embedded with molten paraffin wax. The tissue forms a solid block after the wax cools. Devices known as

microtomes are used to cut the tissue block into sections of 3-5 μm thick. The section is placed on a glass slide, stained and lastly covered by a cover slip. The specimen is ready for histological examination [17, 18].

Diagnostic evaluation of tissue is largely based on a thorough examination of sections stained with hematoxylin and eosin (H&E). Hematoxylin is basic and binds to nuclear material that are acidic and negatively charged, staining them violet. On the other hand, eosin is acidic and binds to positively charged protein side chain, staining them pink.

Other special stains may be required to identify features that are not easily seen on an H&E stain. This study additionally uses Masson's trichrome (MT) stain, another common stain applied to liver specimens during clinical evaluations. The stain specifically highlights type I collagen fibers and imparts a blue colour to the fibers. It is useful in quantifying and staging the stage of liver fibrosis. Hepatocytes and cytoplasmic structures are stained pink while nuclei are stained dark red or black.

The next stain used in this study was immunohistochemical staining (IHC). In any IHC examination, a particular antibody, known as the primary antibody, is used to identify the protein of interest, through a specific antigen-antibody reaction. Subsequently, an enzyme conjugated secondary antibody – which reacts specifically with the primary antibody – is introduced to the specimen. The conjugated enzyme catalyses a chromogenic reaction and produces a colour signal wherever the specific antigen–antibody reaction has taken place. These colour signals are observed under a light microscope [19, 20].

Regeneration of Liver

In healthy livers, hepatocytes remain quiescent, replication activity is low and matches the low prevalence of hepatocyte apoptosis observed clinically. During an injury, the liver has enormous capacity to regenerate, where reconstitution of functional liver mass is completed within weeks of partial hepatectomy (surgical removal of the liver). As such, the two-third hepatectomy model of mice and rats, reflecting acute injury to the liver, is commonly used for the study of regenerative molecular medicine.

Regeneration of the liver can largely be attributed to enhanced hepatocyte proliferation. In partial hepatectomy, DNA synthesis and the mitotic index are enhanced in the remaining liver in relation to the removal of tissue volume. Animal studies demonstrated that DNA synthesis in mature hepatocytes begins 24 hours after partial hepatectomy and the hepatocyte mitotic index increases to as high as 13-fold within the initial 72 hours [21, 22].

In cases of chronic disease or severe acute injury to the liver, proliferation of hepatocytes is either impaired or insufficient to regenerate liver volume adequately. Differentiation and multiplication of liver stem cells come into play to replace the damaged hepatocytes. A stem cell is an undifferentiated cell capable of self-renewal and generating one or more types of specialized cells. Characterized by its histology, oval cells are adult liver stem cells that reside in the small terminal bile ducts. Oval cells are shown to be the progenitor for hepatocytes and bile duct cells. Oval cell activation is observed in majority of chronic human liver diseases and the degree of progenitor cell activation correlates with the amount of inflammation and damage.

Several recent studies are exploring how oval cells can be used as a treatment for liver diseases. Sources of oval cells studied included bone marrow cells and re-programming of hepatocytes. However, oval cells were found to be directly associated in the histogensis of hepatocellular carcinoma (HCC) and its markers were associated with worse prognosis and more recurrences after surgical treatment. It is widely accepted in the field that more needs to be understood before oval cells can be used as a form of stem cell therapy [23-26].

A well-known mitogenic signal in liver regeneration is hepatocyte growth factor (HGF). HGF has been shown to increase 10 to 20 folds in serum after partial hepatectomy. HGF is consumed during the first 3 hours of PH and new HGF are synthesize within 48 hours. In cell cultures, HGF is observed to cause strong mitogenic responses and clonal expansion of hepatocytes. It is produced by other organs, such as the lung and spleen, though the liver is the largest contributor. Its receptor, c-met, is expressed in most cells and facilitates all the effects of HGF. Animal studies also show that the HGF/c-met signalling pathway is irreplaceable in the process of liver regeneration. C-met absent mice were more vulnerable to hepatectomy while surviving mice displayed numerous areas of necrosis and signs of chronic liver damage.

There is no one single factor the mediates the progression of liver regeneration. Other signals include interleukin-6 and epidermal growth factor. Termination of liver regeneration is also an organized process. Regenerated liver volume typically falls within 5% to 10% of the original volume before hepatectomy. TGF-1 is a known suppressor of hepatocyte proliferation. Its expression increases within 5 hours after partial hepatectomy and acts in an antagonistic

action against HGF to control the rate of restoration, where it remains elevated in serum until the end of liver regeneration [27-31].

Fibrosis and Cirrhosis

Despite having multiple growth signals and pathways for inducing liver restoration, the regenerative capacity of liver cells is limited. This is observed through chronic liver diseases in which hepatocytes do not replicate normally, significantly activating oval cells as a result. A plausible explanation for the impaired hepatocyte regeneration is the shortening of telomeres. Telomeres are simple tandem nucleotide repeats that are located at each end of chromosomes. They do not encode for any gene product, but serves to cap and protect the chromosomal ends from DNA damage. Due to the limitation of DNA polymerase, telomeres shorten by 50–100 base pairs after each cycle of cell division in human cells. Upon reaching a critical short length of telomeres, the cell undergoes a permanent cell cycle arrest, known as senescence. Telomerase is an enzyme that serves to synthesize new telomere sequences but remains active only in immature germ cells and certain stem and progenitor cells in adults. despite the reactivation of telomerase in chronic liver diseases, accelerated telomere shortening is still observed, surpassing the synthesis of new base pairs at the ends of the chromosomes.

Recent literature shows that healthy livers contain a high percentage of hepatocytes with multiple sets of chromosome (polyploidy), reflecting the complexity and adaptability of the liver. Furthermore, hepatocytes enlarge in cell size (hypertrophy) as the first step of compensatory response after partial hepatectomy. On the other hand, polypoidal and enlarged hepatocytes are found to be significantly higher in numbers in chronic liver diseases. Enlarged

hepatocytes lead to the production of portal hypertension, a symptom commonly associated with chronic liver disease. This highlights the role of telomeres in hepatocyte regeneration as de-protection of telomeres has shown to lead to higher rates of polyploidization and DNA replication without cell division contributes to cellular hypertrophy [21, 32-35].

Hepatic fibrosis is often the outcome of prolonged impaired regeneration. This is characterized by the deposition of excessive extracellular matrix as part of the regenerative response, due to the hyper-activation of the hepatic stellate cells. Stellate cells are activated upon injury to the liver and transdifferentiate into myofibroblast-like cells. These cells deposit extracellular collagen, forming temporary scars to contract the injured sites. They also promote regeneration and angiogenesis by secreting cytokines and growth factors. After healing is complete, apoptosis takes over to remove the temporary scars. However, in chronic liver diseases, hepatic stellate cells are activated more rapidly and aggressively, resulting in widespread scar formation [36-38].

With the presence of iterative damage, such as chronic hepatitis or alcoholic abuse, the fibrotic process progresses and worsens. Nodule formations are resulted and eventually, leads to late-stage scarring, known as cirrhosis. Cirrhosis is characterized as the loss of lobular structure and internal liver vascular supply is compromised. It is highly debated in the field regarding the reversal of cirrhosis. Clinical cases and animal studies has shown the regression of fibrosis after the cause of injury is removed. However, the loss of lobular architecture has shown to be permanent in cirrhosis despite improving hepatic functions after intervention [22, 39-43].

The only current effective treatment for patients with end-stage cirrhosis is a liver transplant. However, not all patients are suitable for liver transplantation. Essentially, the patient must be able to survive longer with transplantation compared to without transplantation. Due to the limited supply of donors, several grading models were created to prioritize recipients and allocation of donor organs. Compatibility of blood groups, quality and size of donor liver are additional considerations as well. After which, long-term immunosuppressive regimes are administered to prevent transplant rejection. These challenges are pushing clinicians and researchers to search for alternate therapies for chronic liver diseases [44-47].

Alternate Therapies for Liver Diseases

Besides transplanting the donor liver, clinicians had also tried transplanting with hepatocytes, isolated from livers that are unused or deemed unsuitable for transplantation. Hepatocyte transplantation in humans has met with varied success, largely dependent on the disease state. Nevertheless, donor availability is the crucial limiting factor and stem cell-derived hepatocytes are being investigated for this cause [48-50].

According to a report conducted by EuroStemCell on the trend of stem cell research, it was estimated that there were close to 100,000 active stem cell researchers globally in 2012. 47% of stem cell publications were linked to regenerative medicine. A group of researchers attempted to treat liver fibrosis in mice using mesenchymal stem cells (MSC) derived from bone marrow. However, bone marrow as a source of stem cells has its disadvantages. In clinical bone marrow transplant, the donor is often put under general anaesthesia, posing some form of risks to the donor. This had led other

researchers to look for alternate sources of MSC, such as Wharton's Jelly, from the umbilical cord, which is often discarded after giving birth.

While results using MSC are promising, the development to hepatocytes are highly controversial. Mesenchymal cells are non-polarized cells, capable of moving as individual cells, lacking intercellular connections. Epithelial cells, like hepatocytes, are adherent cells that attach to each other, forming coherent layers exhibiting apical-basal polarity. It is believed that MSC undergo mesenchymal to epithelial transition and form hepatocytes in treating the injury, which is not yet well understood [51-54].

Cord Lining Epithelial Cells (CLEC)

The dilemmas associated with the ethical and social issues of potential stem cell therapies must be thoroughly examined to ensure that science remains as the vehicle for hope and not harm. Our research ultimately aims to use HLC as an alternate therapy for liver diseases by enhancing liver regeneration. This can be achieved via two ways, through trophic factors that repair cellular damage and, replacing damaged hepatocytes and its functions.

As mentioned above, the umbilical cord is an attractive source of stem cells, as it is usually discarded as bio-waste accompanying the delivery of a new-born. The absence of risks to either mother or child makes it ethically acceptable. Furthermore, the supply of umbilical cords is highly sustainable. CLEC was discovered by the group led by Phan in 2003 when they cultured umbilical cord amniotic membrane in modified keratinocyte medium [55]. It was estimated that a single umbilical cord could yield 6 billion CLEC at passage 1, far

exceeding the MSC that could be derived from bone marrow, cord blood, and adipose tissue.

CLEC possess properties of both epithelial cells and embryonic stem cells. The cells were tested positive for MUCIN1, whose function is to protect the epithelium by binding to pathogens; CD151, involved in epithelial cell-to-cell adhesion; p63, an adult epithelial stem cell marker and CK7, CK14 and CK19 in varying degrees. Furthermore, cells were positive to several embryonic stem cell markers, such as Oct-4, Nanog, ring-exported protein-1 (REX-1), SOX-2, telomerase reverse transcriptase (TERT), and SSEA-4.

This had led Phan and team to further explore the clinical applications of CLEC. CLEC was found to closely resemble primary neonatal epidermal keratinocytes, showing its potential in tissue-engineered skin grafts [56]. The team investigated the transplantation potential of CLEC in immuno-competent mice [57]. CLEC were maintained for extended periods compared to human epithelial cells serving as control (see Figure 5).

In another study, CLEC was seeded on human amniotic membrane and transplanted onto limbal stem cell deficient rabbits [58]. The tissue-engineered cell sheets successfully regenerated the damaged cornea surface and histological examination revealed that the cellular organization in the transplanted eyes resembled that of normal healthy cornea epithelium (see Figure 6). Due to its multi-potency and immunosuppressive qualities, CLEC was also studied as potential bio-implants for safe and long-term secretion of anti-hemophilic factor in hemophilic patients [59].

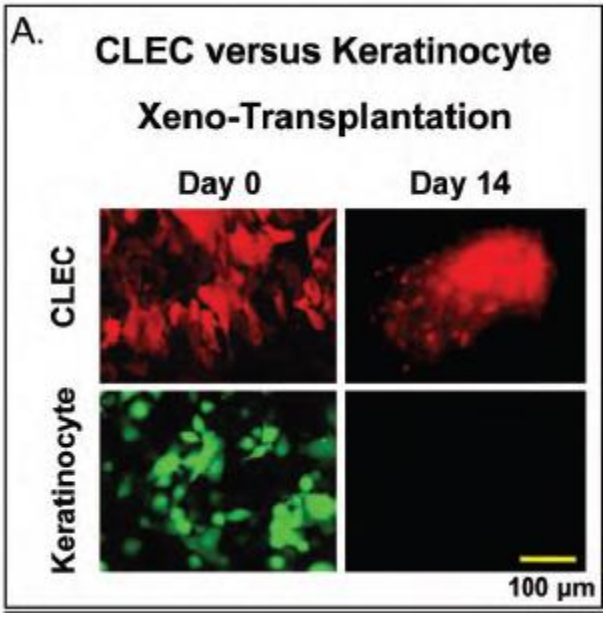

Figure 5: CLEC surviving in xeno-transplant host up to 2 weeks. CLECs and keratinocytes were transfected to express DsRed2 and eGFP respectively under fluorescent microscopy. At 14 days after transplantation, red fluorescence indicates the presence of CLECs while green fluorescence of normal human keratinocytes was not detected. Image taken from [57].

This study initially started out looking at alternative sources for *in-vitro* drug metabolism model. HLC were differentiated from CLEC to serve as a novel *in-vitro* drug biotransformation study model [60]. HLC were found to develop morphological changes, glycogen storage abilities and metabolic capabilities, such as albumin production and cytochrome P450 expression. Other studies had suggested culturing isolated hepatocytes on extracellular matrix such as collagen, improved hepatocyte maturation and functions [61, 62].

For non-embryonic stem cells, CLEC have shown to overcome the pre-existing difficulties inherent to other stem cells, like MSC harvested from bone marrow and Wharton's Jelly. Umbilical cord lining offers a realistic, practical and affordable alternative source of stem cells for tissue repair and regeneration.

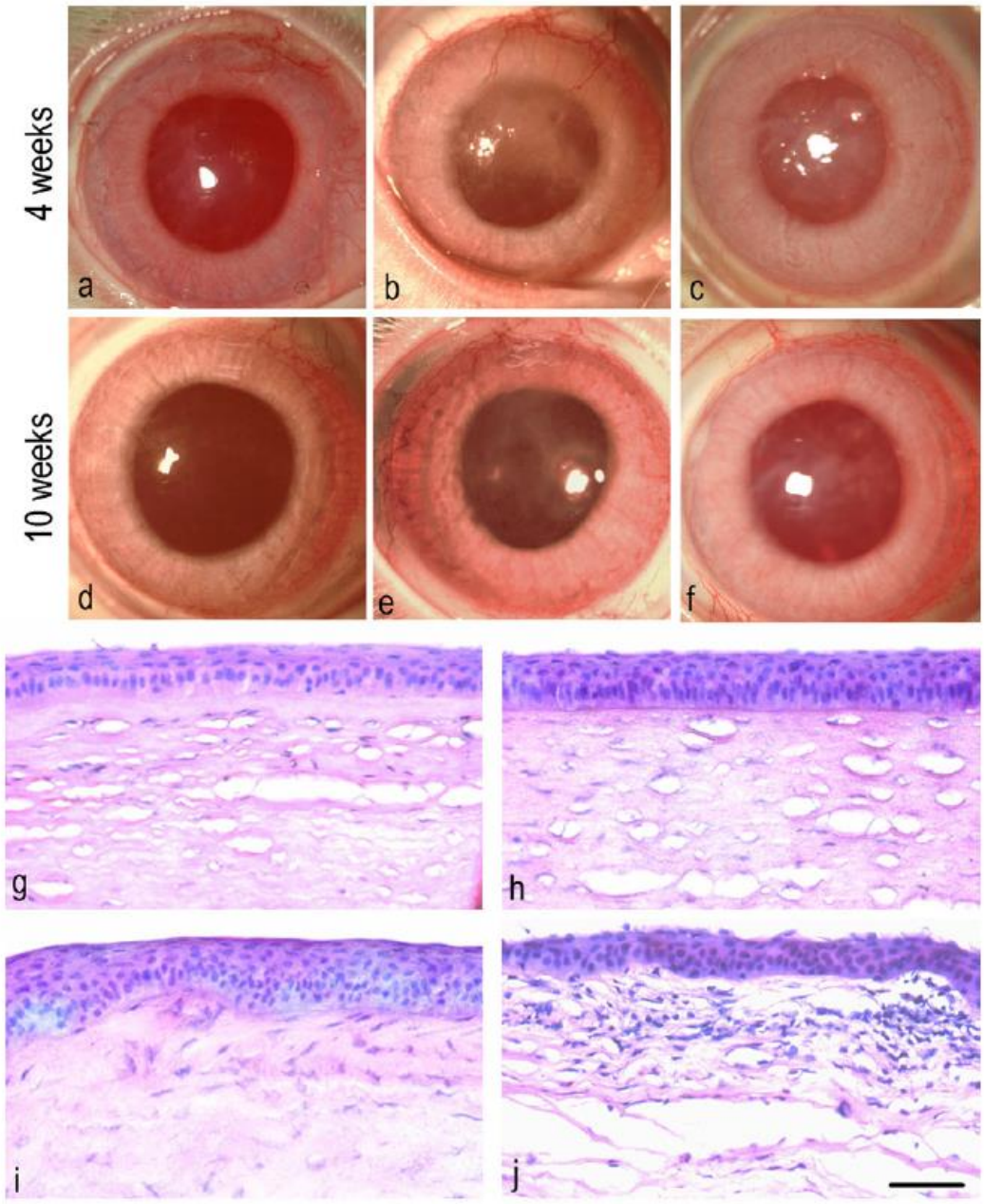

Figure 6: Effects of transplanted CLEC on rabbits' corneal surface. (a & d) Damaged corneal with CLEC transplanted showed little opacity after 4 weeks and no opacity after 10 weeks. (b & e) Control membrane transplanted eye showed significant opacity in cornea after 4 weeks, with reduced opacity after 10 weeks. (c & f) Eye with no transplant eyes exhibited opacity and neovascularization in cornea after 4 and 10 weeks respectively. (g) H&E staining showed regular smooth corneal epithelium for CLEC transplanted eye. (h) Normal structure of un-treated corneal epithelium. (i) Thick corneal epithelium with some infiltrating cells for eye with no transplant. (j) Irregular corneal epithelium with many infiltrating cells in stroma for control membrane transplanted eye. Bar is 100 μm in length and image taken from [58].

Methodology

Source of CLEC

Human umbilical cords were collected with informed consent of the mothers after normal deliveries. The Wharton's jelly and blood vessels were separated from the umbilical cord amniotic membrane by dissection. The isolated umbilical cord lining was cut into small pieces and explanted onto tissue culture dishes. The umbilical cord amniotic membrane was isolated by dissection, and explanted onto tissue culture dishes with proprietary medium, PTTe1, made up of Medium 171 supplemented with 2.5% v/v FBS, 50 µg/mL insulin-like growth factor-1, 50 µg/mL platelet-derived growth factor-BB, 5 µg/mL transforming growth factor-b1, and 5 mg/mL insulin.

Low passages (1 or 2) of CLEC were selected for single-cell cloning. Colonies formed from single cells were monitored for 12 days and tested for hepatic stem cells makers. A small portion of cells were tested using immuno-staining assays for AFP, CK19, CK18 and Albumin. Cell colonies with high expression of hepatic stem cell markers of 60% and above were chosen for hepatogenesis.

Hepatogenesis

The chosen cell colonies were plated at a density of 5,000 cells/cm^2 and cultured at 37ºC in an atmosphere of 95% air and 5% carbon dioxide. Upon reaching confluency at passage 3 or 4, the PTTe1 medium was replaced with hepatocyte culture medium (HCM™ Bulletkit®, Lonza). The CLEC colonies were cultured in HCM for 14 days, followed by hepatocyte maintenance medium (HMM™, Lonza) for another 14 days to differentiate into HLC. The media was refreshed every 2 to 3 days.

Liver Insufficient Porcine Models

50% left hepatectomy procedure – removal of 2 left most liver lobes – were performed on adult porcine to create a liver insufficiency animal model. 16 Yorkshire-Dutch Landrace pigs, with a mean weight of 40.5 kg on day of surgery, were initially selected for this study. All pigs were tranquilized by intramuscular injection of ketamine (1 mg/kg). General anaesthesia was subsequently induced using 5% isoflurane and maintained at 3% isoflurane until the entire surgery was completed.

The pigs were placed in supine position and the abdomen opened through a subcostal incision extending from the right anterior axillary line to the left mid-axillary line, plus a midline incision from 2 cm above the xiphisternum to the transverse incision. Surgical tools were inserted into the body via laparoscopic ports (see Figure 7). The liver was mobilized by division of peritoneal reflections to the diaphragm and division of the falciform ligament. Subsequently, the left triangular ligament and the lesser omentum were divided to completely mobilize the left liver lobes. The parenchyma was lastly divided after control of inflow and outflow to each lobe.

Novel Stem Cell Delivery Method

After the two lobes were resected and removed, 2 pieces of 50 x 50 mm collagen scaffold (HealiAid® Collagen Wound Dressing, Maxigen) were directly applied on the cut liver surface. Figure 8 shows how the scaffold was applied.

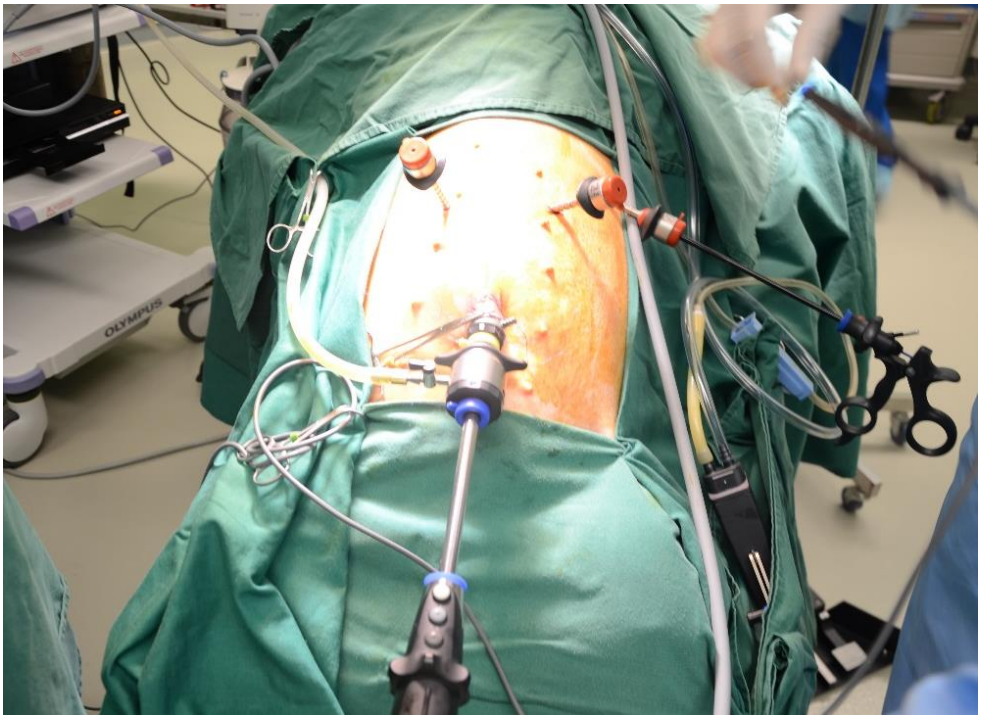

Figure 7: Setup for hepatectomy on porcine subject. Insertion of various laparoscopic ports and endoscope on ADD2 subject. Image taken in CM opertating theatre.

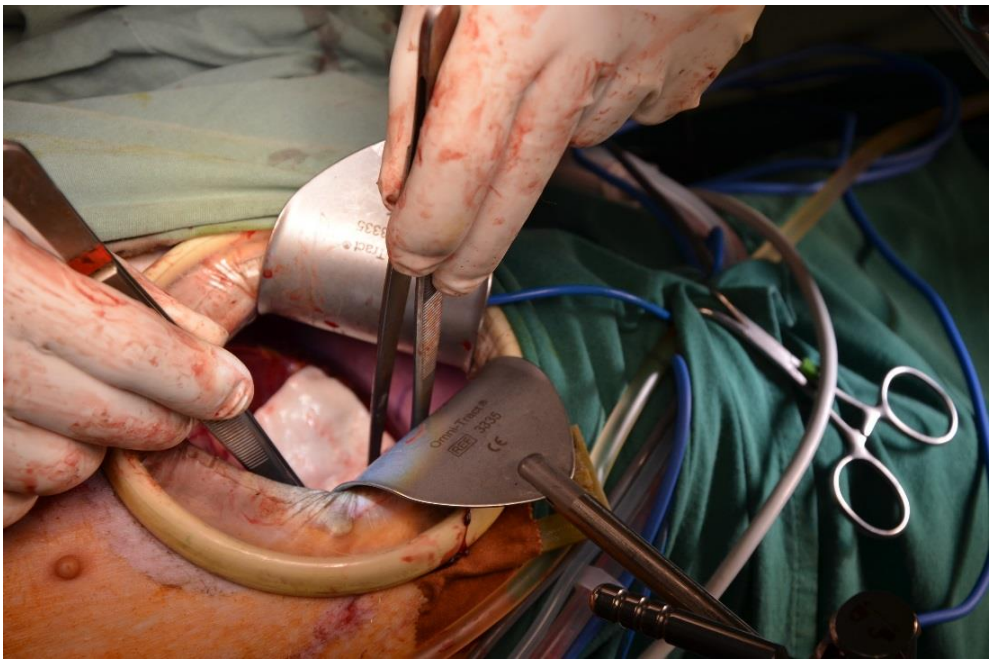

Figure 8: Application of collagen scaffolds onto resected liver surface. Collagen scaffolds were inserted through the same opening the two right liver lobes were removed from.

Prior to application, the collagen scaffold was soaked for 5 minutes in either:

a. 30 ml Normal saline solution (0.9% NaCl). Subjects receiving such scaffold were treated as the control arm. Or,
b. 30 ml HLC solution (see Figure 9). On the day of the surgery, the HLC colony were gently detached from the tissue culture surface with cell scrapers and transported to the operating room. It was estimated that 10 million HLCs were transferred into solution. Subjects receiving such scaffold were treated as the study arm.

After soaking, 10 x 10 mm of scaffold were removed and fixed in 10% neutral buffered formalin solution for histological characterization.

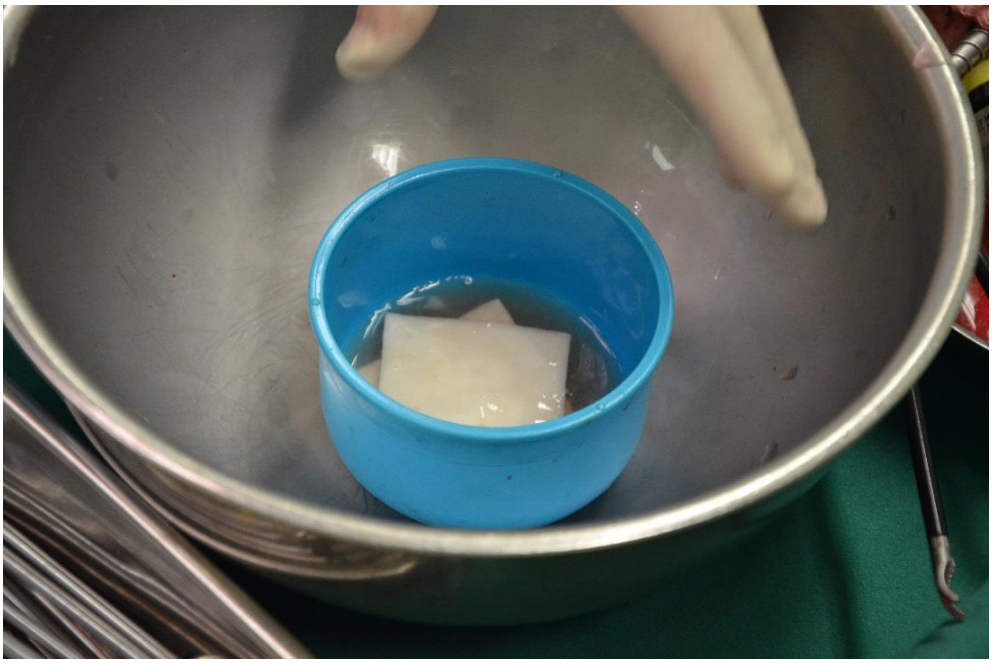

Figure 9: Soaking of collagen scaffolds in its respective solution. Collagen scaffolds were soaked for 5 minutes in either saline or HLC solution on a sterile container. This was performed just before the application of the collagen scaffolds onto the resected surface.

The remaining respective solution were dispensed directly over the resection site, after the collagen scaffolds were applied on the liver surface, using a 20 ml syringe, as shown in Figure 10.

Figure 10: HLC solution in a 20 ml syringe. Remaining solution were extracted with the syringe and dispensed directly over the scaffolds, after being positioned on the resected surface.

Lastly, the abdominal muscles and rectus sheath were closed with 1-0 PDS continuous suture, followed by closing of the skin with subcuticular 4-0 Monocryl. A portal catheter was inserted permanently into the external jugular vein to allow frequent blood collection. Anaesthesia was discontinued and considered completion of surgery. All procedures followed aseptic precautions and were done under the approval of Institutional Animal Care and Use Committee (IACUC).

Post-operative Care

The pigs were housed in individual pens in NUS Comparative Medicine (CM) Vivarium, maintained at 25ºC and ambient humidity, over a post-operative observation period of 21 days. For the first 7 days, the pig was given analgesic (buprenorphine) and antibiotics (enrofloxacin, amoxicillin, clavulanic acid and carprofen) to reduce localised pain and inflammation. The portal catheter was

flushed with 1% heparin w/ normal saline solution every other day for subsequent weeks to prevent deep vein thrombosis.

Blood Examination

10 ml venous blood were drawn from the subjects after the surgery ended (Post-op), day 1 after surgery (POD1), day 2 after surgery (POD2), day 4 after surgery (POD4), day 6 after surgery (POD6), day 8 after surgery (POD8), day 15 after surgery (POD15) and day 21 after surgery (POD21) before euthanasia.

The blood was sent to National University Hospital and examined for PT, INR, ALB, TBIL, DB, IB, AST, ALT, ALP and LDH. The data was subsequently collected and tabulated respectively.

CT and Liver Volumetric Study

CT scans of the liver were performed in NUS CM Imaging Facility, before the hepatectomy (Pre-op), Post-op, POD8 and POD15. The subjects were under general anaesthesia throughout the scans. Triple phase liver CT protocol was performed.

Images from contrast-enhanced portal venous phase were extracted and sent to I^2R for data processing. The liver volume was determined and tabulated respectively. On POD21, after the pig was euthanized via pentobarbital (150 mg/kg), the liver (without the gallbladder) was harvested and its volume measured via water displacement method. The measured volume was increased 13% to account for blood perfusion compared to CT-determined measurements. The results were tabulated respectively.

Histological Procedures

On POD8 and POD15, CT-guided core needle biopsy was performed respectively, after the completion of the CT scan. The procedure was carried out by CM veterinarian, using a 16G 15 cm long percutaneous biopsy instrument (Temno Evolution®, Carefusion). The subject was placed in left lateral recumbancy and the biopsy needle was inserted between the right lower ribs. 40 mm^3 core liver tissue was removed from the subject. CT images were referenced to prevent injury to major vessels. The core tissue was then sent for fixation in 10% neutral buffered formalin solution.

On POD21, after water displacement volume measurement, the site where the collagen scaffolds were placed and a peripheral site away from the collagen scaffold (yellow circles in Figure 11), were removed from the rest of the liver via a #10 scalpel blade and immersed in 10% neutral buffered formalin solution for fixation.

Tissue fixation was carried out for a minimum of 48 hours before sending to A*STAR Advanced Molecular Pathology Laboratory for automated tissue processing. This included processing fixed tissue into paraffin-embedded blocks, sectioning blocks into 5 µm thick samples and placing samples onto glass slides. For every block, one slide of H&E stained and one slide of MT stained slide were requested.

Anti-Human Nuclei Staining

Anti-nuclei human antibody (Merck Millipore, MAB1281) was used as the primary antibody. IHC staining was carried out on selected paraffin sections,

according to protocol attached in Appendix A. Micrographs were taken and analysed respectively.

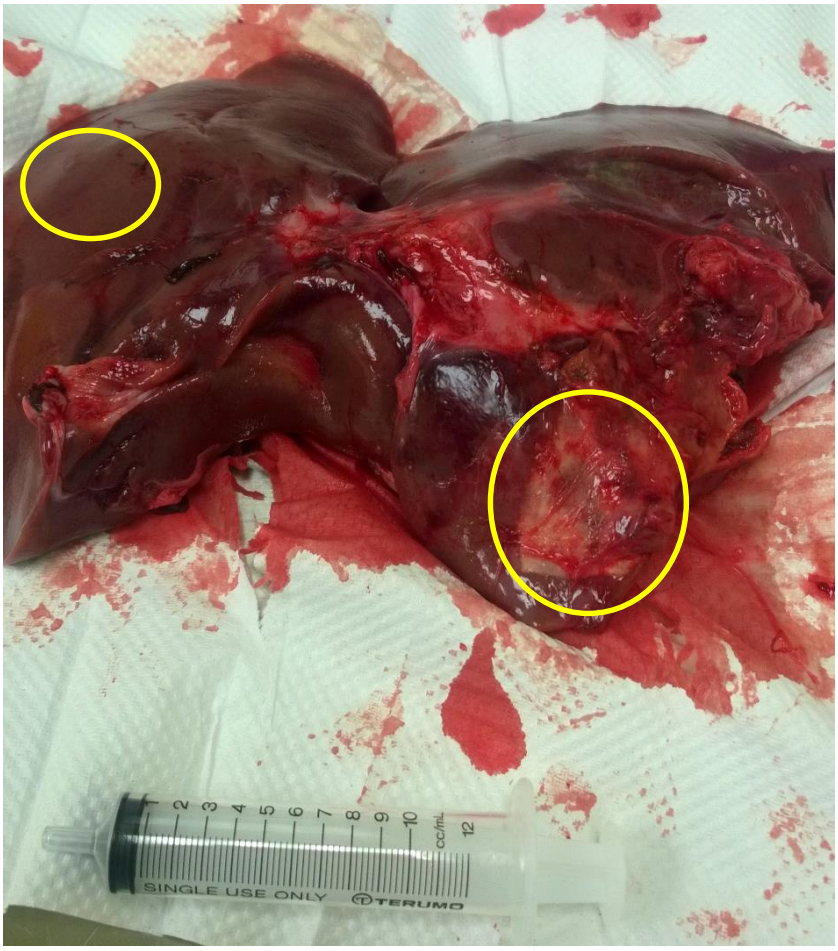

Figure 11: Excised liver after subject's euthanasia. Excised liver was used in volumetric measurement and selected sites (circled in yellow) were removed and sent for hisotogical examinations. The partially absorbed collagen scaffold is clearly visible in the right yellow circle. 10 ml syringe was used as scale.

Results

Subject Profiles and Outcomes

Due to the complexity in performing the 50% hepatectomy procedure on porcine models, only 11 out of 16 pigs (68.8%) were able to be transplanted with the respective collagen scaffolds. The remaining pigs suffered mortality amidst the surgery due to uncontrolled intraoperative blood loss. These pigs were omitted from the analysis of this study. Table 1 shows the profile and outcome of the 11 pigs that were transplanted with collagen scaffolds.

Table 1: Overview of subjects' details and post-operative survival.

Subject Name	CM ID.	Sex	HLC Implanted	Weight on Surgery (kg)	Mean Weight (kg)	POD Survival
CARE9	496089	M	x	43.1	40.0	21
CARE12	10000	M	x	42.0		21
ADD2	1096	F	x	34.0		21
ADD3	1098	F	x	41.0		16
CARE10	496090	M	✓	38.0	40.8	21
CARE11	496088	M	✓	50.4		21
CARE14	9999	M	✓	41.8		15
ADD4	7006	F	✓	39.0		21
ADD6	0069	F	✓	42.6		21
ADD7	1123	F	✓	42.0		21
ADD9	1163	F	✓	32.0		21

Both sexes were equally represented in both treatment groups while the weight difference between the two groups on the day of the surgery was 0.8 kg (2%). One subject from the control group and the study group suffered from ascites and were euthanized on post-operative day 16 and day 15 respectively. CM veterinarians attributed the cause to be intestinal adhesion and obstruction. All other subjects were euthanized at study end point of post-operative day 21.

Statistics

To show statistical differences between the two different groups with a large enough effect size and statistical power, a sample size of 60 porcine models is required with 30 in each group. The calculation is shown in Figure 12. This initial study serves as an abridgement to the larger sample size study and assumes that the samples drawn are from the same intended porcine population.

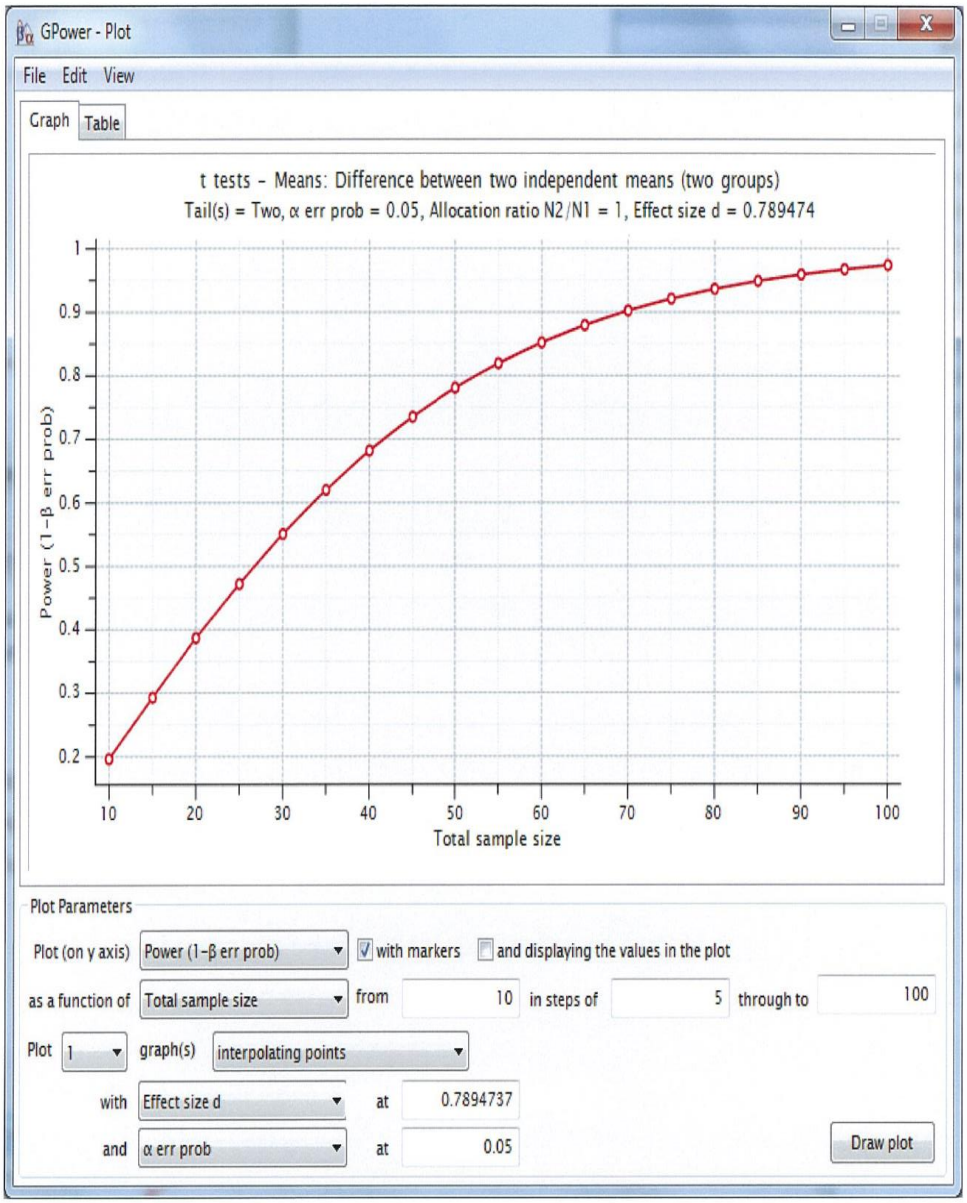

Figure 12: Graph of sample size calculation. A sample size of 60 is required for 85% statistical power and 0.79 effect size.

DeRitis Ratio

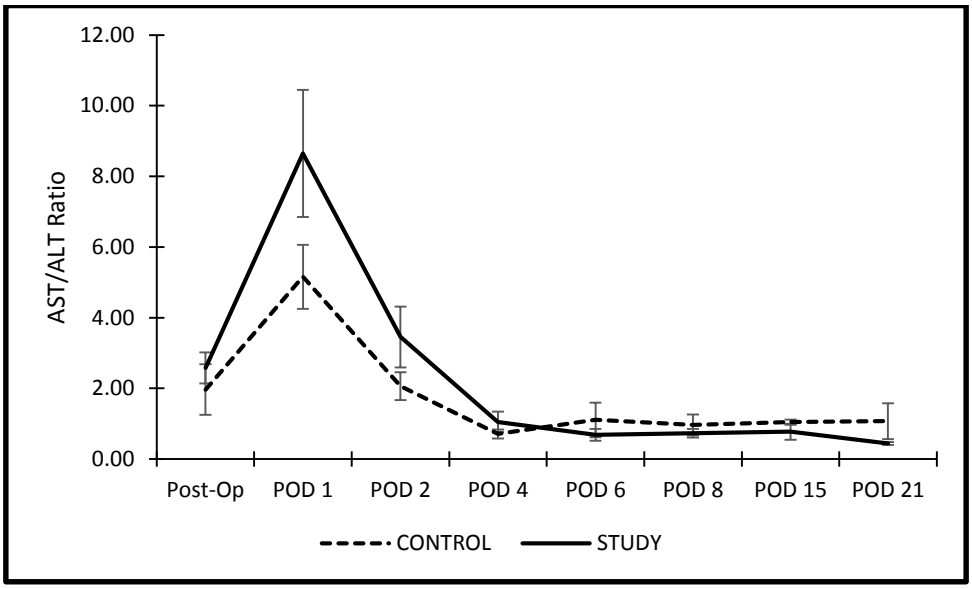

Figure 13: Graph of DeRitis ratio for 21 days after hepatectomy. Comparison of average DeRitis ratio between control and study group. Error bars represents one standard error. Raw data is found in Appendix B.

Figure 13 shows the average DeRitis ratio of both groups for 21 days after the surgical procedure. Both groups had elevated DeRitis ratio after hepatectomy, with the peak ratio taking place on the subsequent day of surgery. The ratio of both groups dropped significantly and plateaued after post-operative day 4 to post-operative day 21. Performing a two sampled t-test with unequal variances, means of both groups were found not to be statistically significant (p >0.05). DeRitis ratio is used to indicate the extent of cellular necrosis and how fast the liver recovers from the fall of the ratio values. Hence, it is observed that both groups started liver recovery after post-operative day 4 with no statistically significant difference in the rates of recovery between the two groups.

Prothrombin Clotting Time

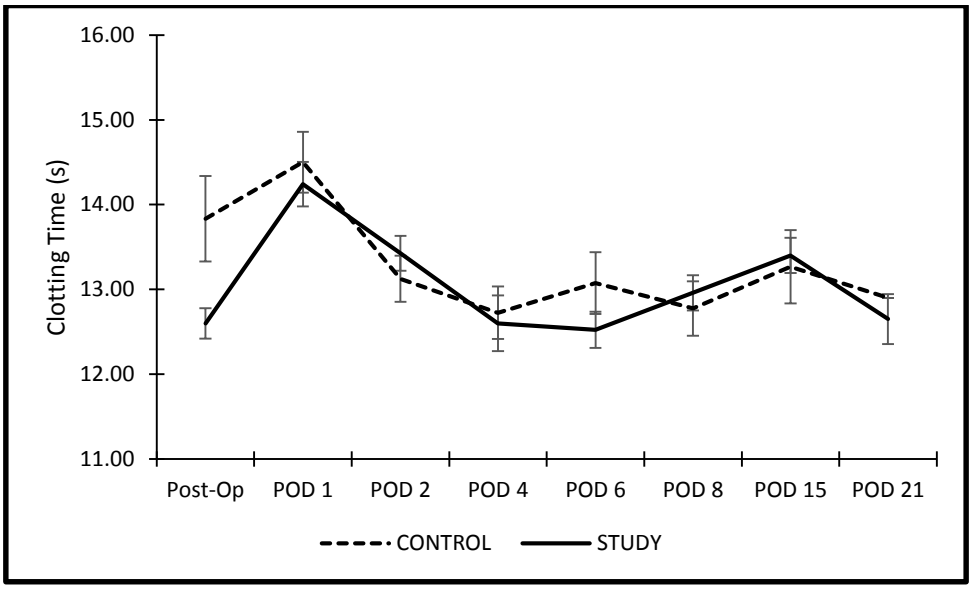

Figure 14: Graph of prothrombin clotting time for 21 days after hepatectomy. Comparison of average clotting time between control and study group. Error bars represents one standard error. Raw data is found in Appendix B.

Figure 14 shows the average prothrombin clotting time of both groups for 21 days after the surgical procedure. Both groups had peak clotting time at the subsequent day of surgery (>14 s) and the clotting time for both groups fall and stay within the range of 12.5 -13.5 seconds up to post-operative day 21. Performing a two sampled t-test with unequal variances, means of both groups were found not to be statistically significant (p >0.05). Prothrombin clotting time is used to indicate the synthetic capability of the liver. With approximately 50% of the liver volume removed, the synthetic function of the liver is expected to be impaired. This is shown in the peak value at POD1 for both groups. However, this quickly drops for both groups with no statistically significant difference between both groups. Furthermore, suggesting that 50% hepatectomy may not be a damage severe enough to impair the synthetic capabilities of the liver significantly.

Serum ALP Concentration

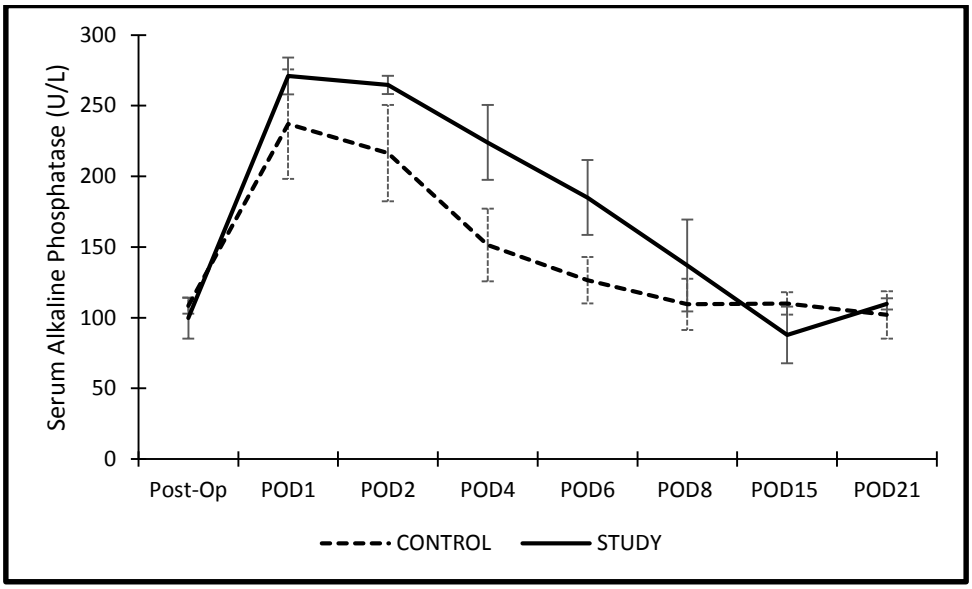

Figure 15: Graph of serum ALP concentration for 21 days after hepatectomy. Comparison of average serum ALP concentration between control and study group. Error bars represents one standard error. Raw data is found in Appendix B.

Figure 15 shows the average serum ALP concentration of both groups for 21 days after the surgical procedure. Both groups had elevated ALP concentration after hepatectomy, with the peak ratio taking place on the subsequent day of surgery. The ALP concentration continued to fall for both groups throughout the post-operative 21 days. Performing a two sampled t-test with unequal variances, means of both groups were found not to be statistically significant ($p > 0.05$). Serum ALP concentration is used to indicate the extent of biliary dysfunction or obstruction. Therefore, it is observed that both groups had impaired biliary function due to the hepatectomy procedure and continued to recover from the damage through the 3 weeks after the surgery with no statistically significant difference between both groups.

Liver Volumetry

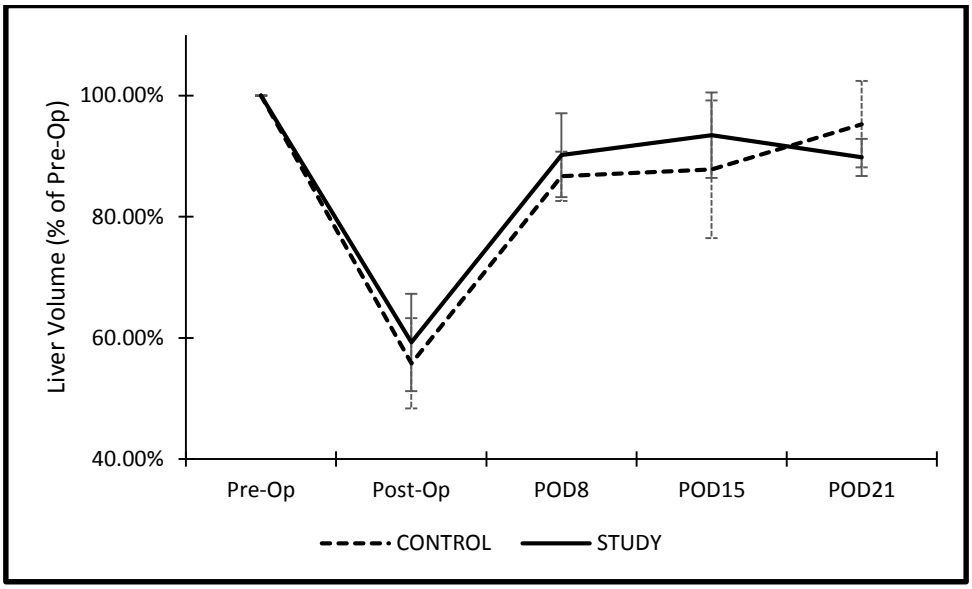

Figure 16: Graph of liver volume before and 21 days after hepatectomy. Comparison of average liver volume (% of pre-Op volume) between control and study group. Error bars represents one standard error. Raw data is found in Appendix C.

Figure 16 shows the average liver volume percentage of both groups as compared to the pre-operative liver volume for 21 days after the surgical procedure. With the removal of two left most liver lobes, approximately 42% of liver volume was excised from the subjects. By the end of the post-operative first week, approximately 46% of liver volume was regenerated for both groups. The liver of both groups then slowly adjusted to the pre-op liver volume till the end of post-operative day 21. Performing a two sampled t-test with unequal variances, means of both groups were found not to be statistically significant ($p > 0.05$). Liver mass reconstitution is an indicator on the rate of regeneration of the liver. Hence, it is observed that there is no statistically significant difference between both groups on their rate of liver regeneration.

Micrographs

Scaffold Characterization

Before the application of the collagen scaffold onto the resected sites, a 10 mm x 10 mm of scaffold after soaking with HLC were removed for histological characterization. Figure 17 shows the wavy thread-like structure of the collagen scaffold structure while Figure 18 shows the epithelial cell characteristics of HLC. Despite the porous structure of the collagen scaffold, it was also observed in Figure 20 that HLC only penetrated the surface of the scaffold superficially. No HLC was found in the inner layers of the collagen scaffold.

Figure 17: H&E staining of collagen scaffold with HLC. Scaffold was soaked in HLC for 5 minutes. The collagen scaffold was observed to have wavy and random threadlike structures. Observed using 4x objective lens.

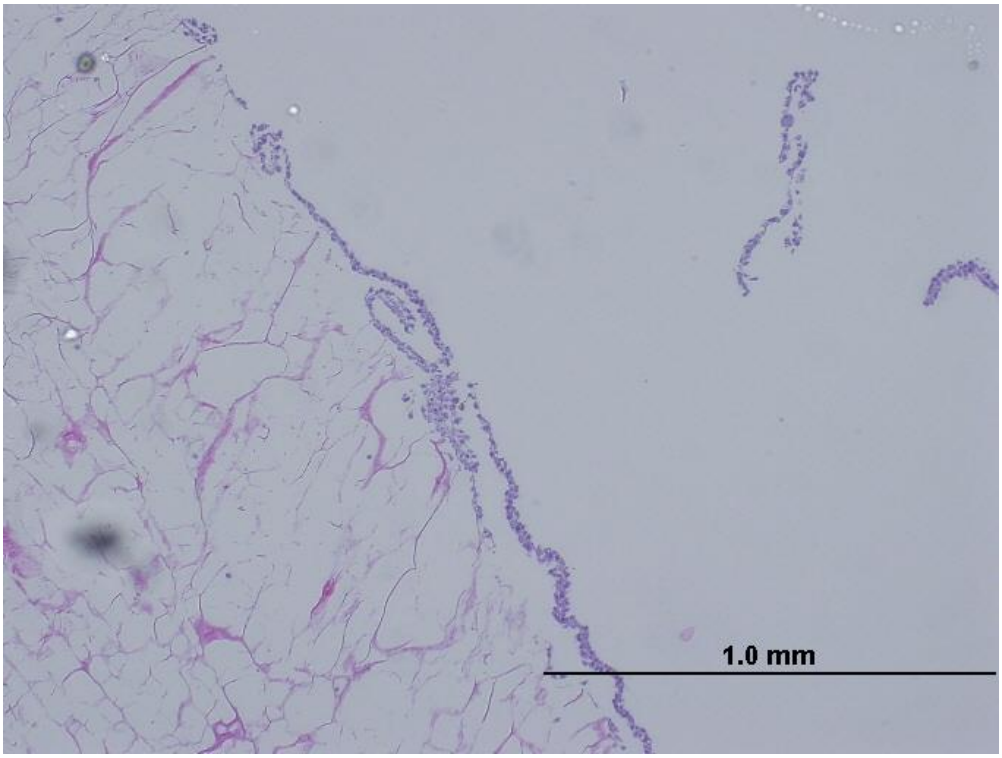

Figure 18: H&E staining of HLC displaying epithelial cell characteristics. Scaffold was soaked in HLC for 5 minutes. The squamous structure of HLC is clearly visible, located at the surface of the scaffold. Observed using 4x objective lens.

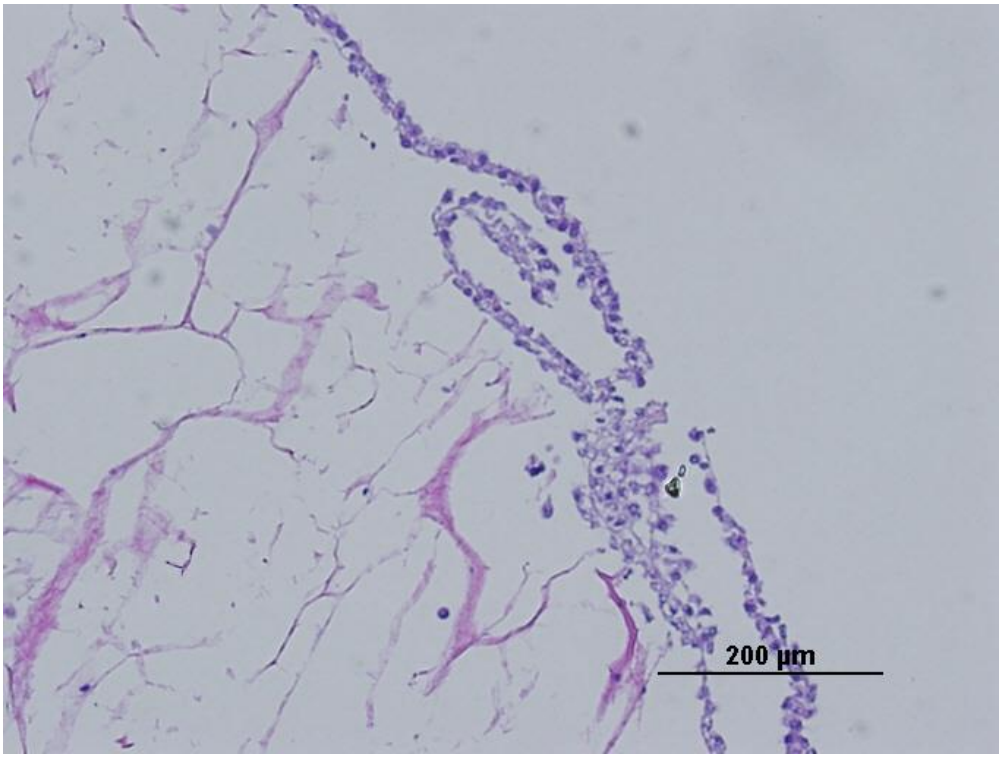

Figure 19: H&E staining of HLC before implantation. Scaffold was soaked in HLC for 5 minutes. The squamous structure of HLC is clearly visible, located at the surface of the scaffold. Observed using 10x objective lens.

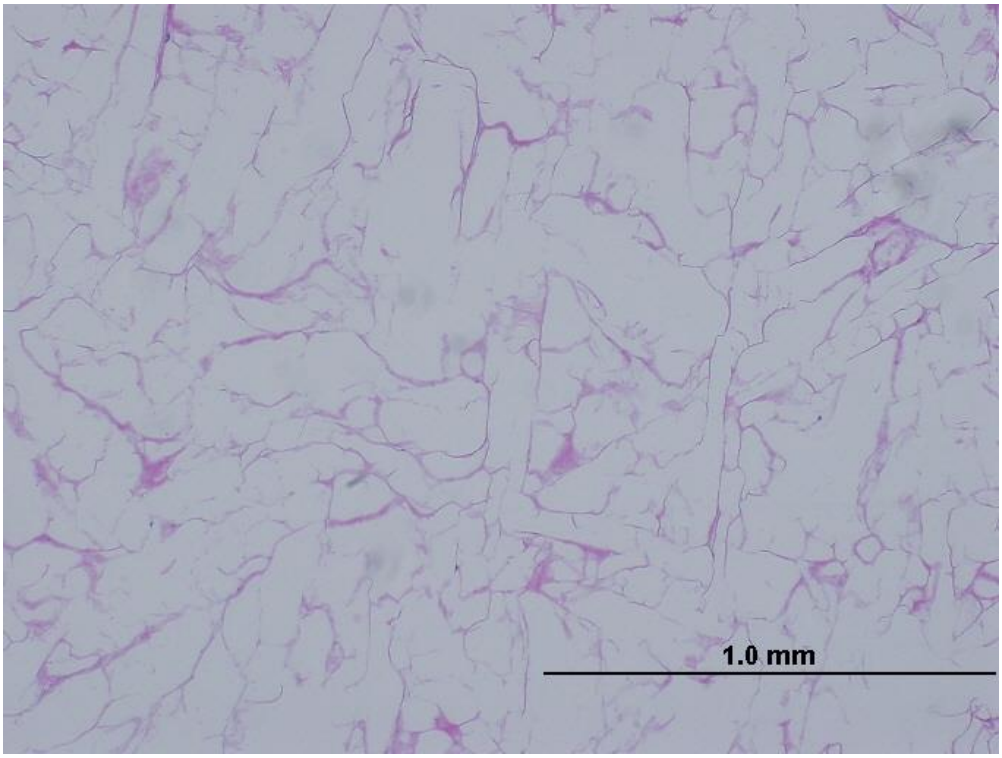

Figure 20: H&E staining on inner layers of scaffold. Scaffold was soaked in HLC for 5 minutes. No HLC was observed in the inner layers of scaffold, suggesting that HLC only penetrated the collagen scaffold superficially. Observed using 4x objective lens.

Masson's Trichrome Staining

To understand how the collagen scaffold is being absorbed by the porcine liver after post-operative 21 days, MT staining is performed on the scaffold-liver or transplant interface. The stain specifically highlights collagen fibers and imparts a dark blue colour to the collagen scaffold fibers. Figure 21 shows the absorption of the collage scaffold into the transplant interface of a subject from the control group. Figure 22 shows the absorption of the collage scaffold into the transplant interface of a subject from the study group. Furthermore, this staining also allow for the localization of human antigens during IHC staining.

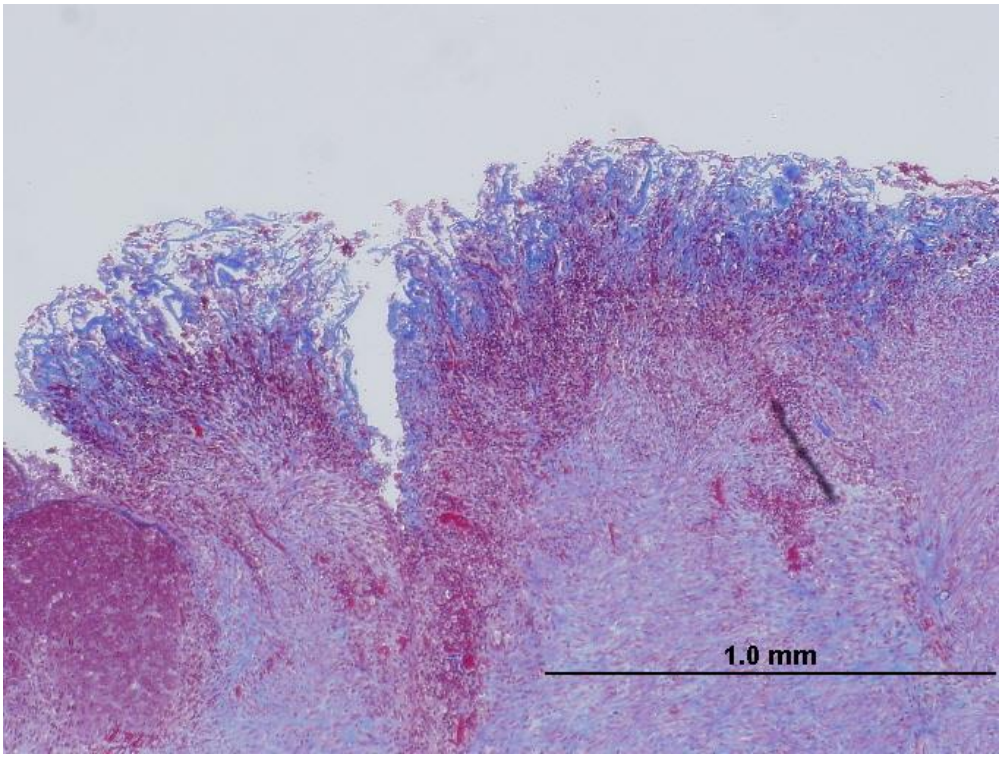

Figure 21: MT staining of collagen scaffold after POD21 in control subject. Section was removed from the scaffold-liver interface in subject ADD2. It was observed that the scaffold was being absorbed into the fibrous tissue of the liver as part of the regenerative process. Observed using 4x objective lens.

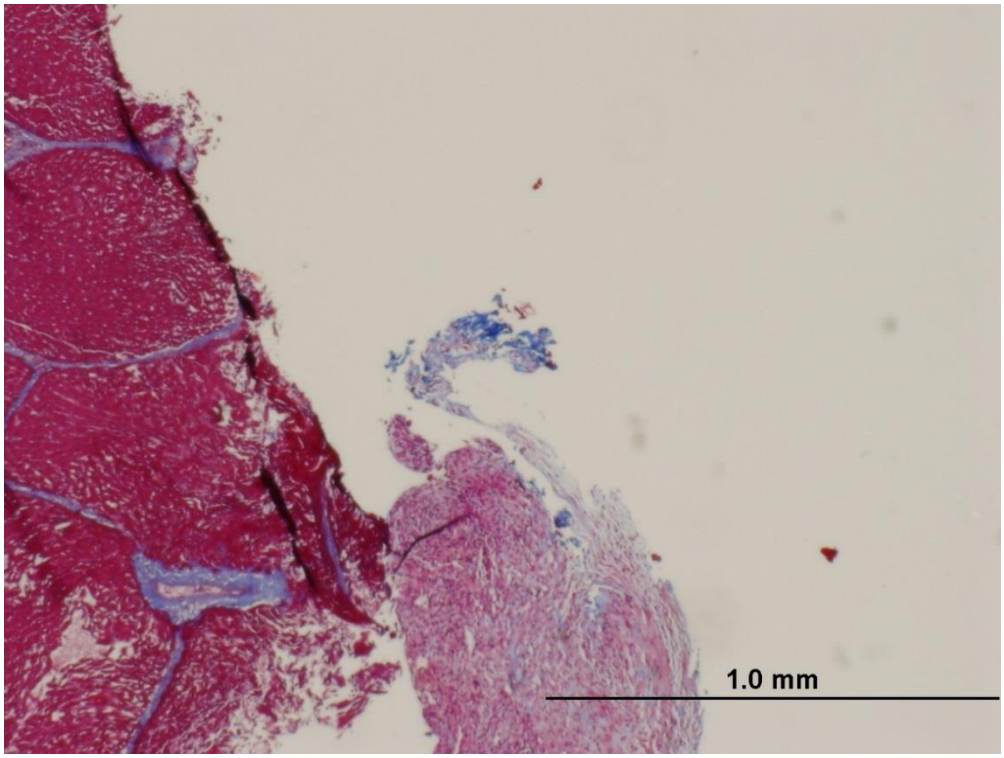

Figure 22: MT staining of collagen scaffold after POD21 in study subject. Section was removed from the scaffold-liver interface in subject ADD4. It was observed that the scaffold was being absorbed into the fibrous tissue of the liver as part of the regenerative process. Observed using 4x objective lens.

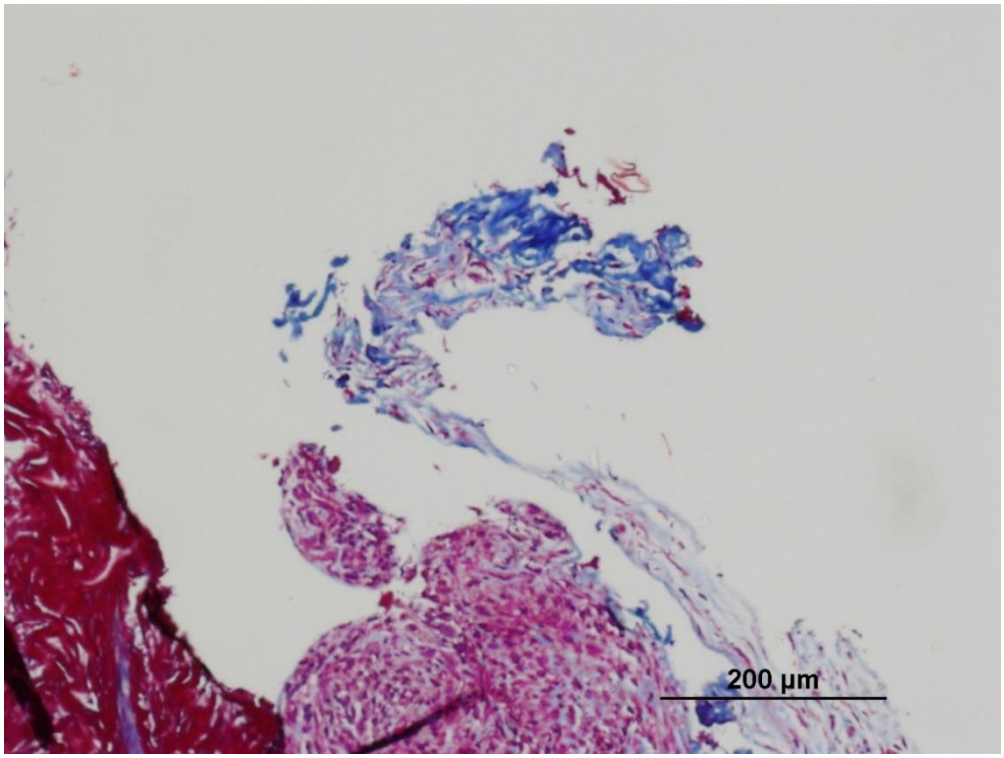

Figure 23: MT staining of scaffold after POD21 in study subject (magnified). Section was removed from the scaffold-liver interface in subject ADD4. It was observed that the scaffold was being absorbed into the fibrous tissue of the liver as part of the regenerative process. Observed using 10x objective lens.

Transplant Interface Observations

The interface between the collagen scaffold and resection margin surface was also studied for both groups. Interfaces of both groups, after post-operative 3 weeks, showed minimal and non-specific reactions. No signs of fatty changes or significant cellular rejection were observed adjacent the interfaces of both groups. Figure 24 shows the interface from a control subject while Figure 26 shows that of a study subject. Healthy liver lobules were observed next to the regenerating fibrous tissue for both control and study groups, shown in Figure 25 and Figure 27 respectively.

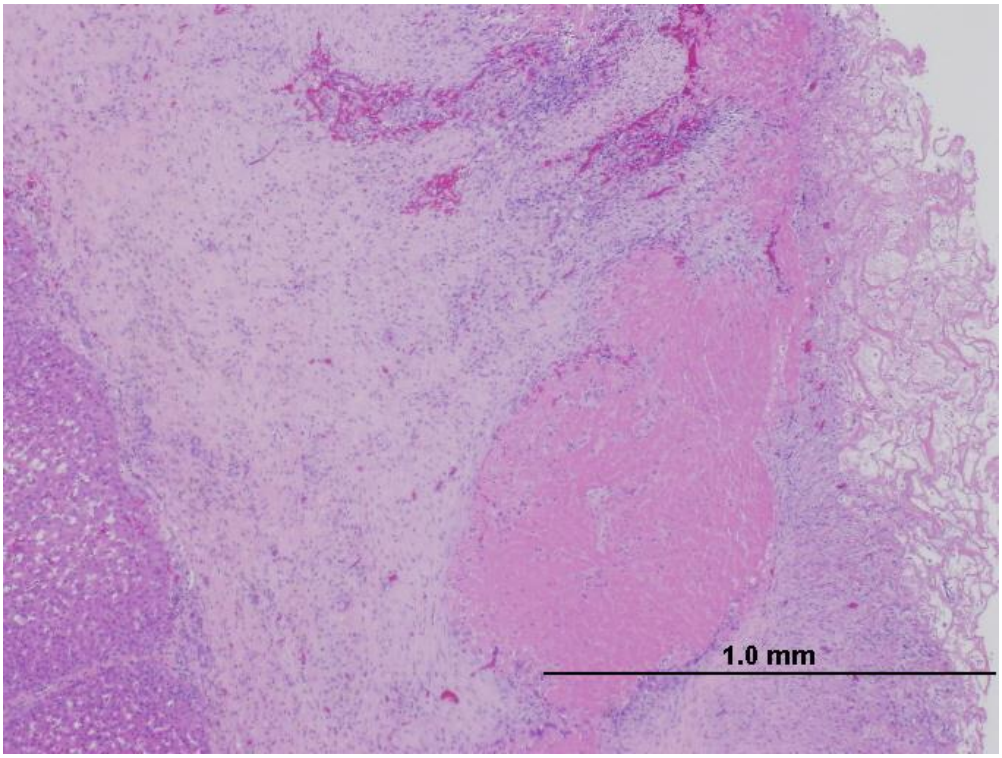

Figure 24: H&E staining of transplant interface after POD21 in control subject. Section was removed from the scaffold-liver interface in subject ADD2. It was observed that the scaffold (extreme right) was being absorbed into the fibrous tissue of the liver as part of the regenerative process. No signs of specific or significant reactions were detected. Observed using 4x objective lens.

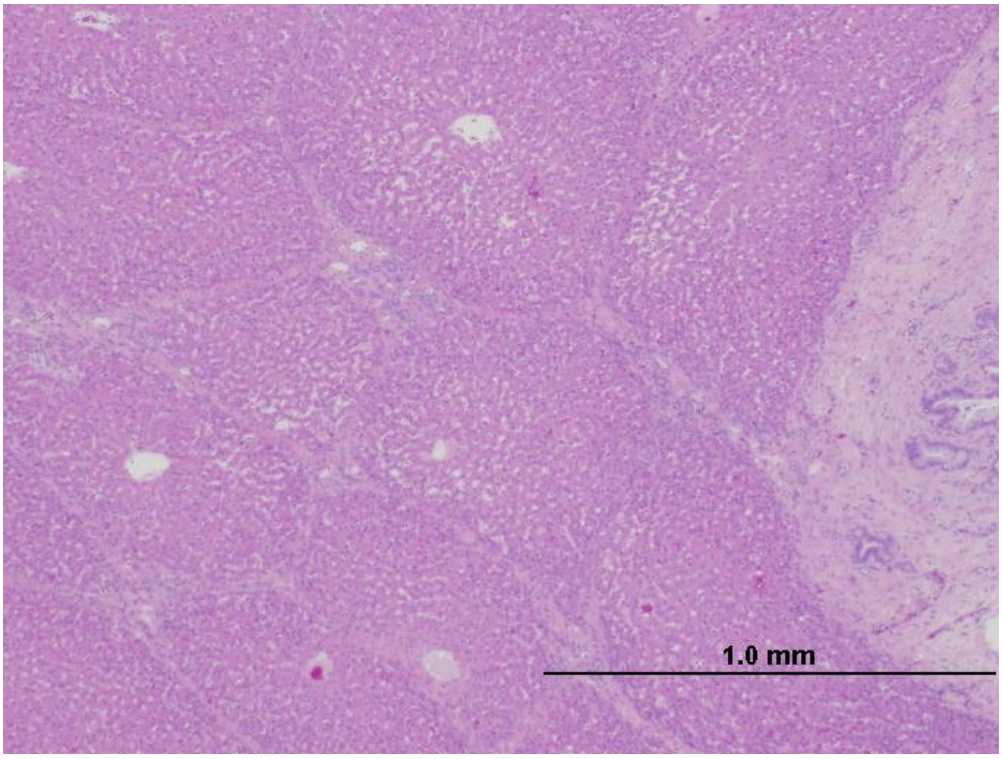

Figure 25: H&E stained lobules adjacent transplant interface of control subject. Section was removed from the scaffold-liver interface in subject ADD2. Healthy lobular structures were seen next to the regenerating fibrous tissue. No signs of fatty changes or cellular rejections were detected. Observed using 4x objective lens.

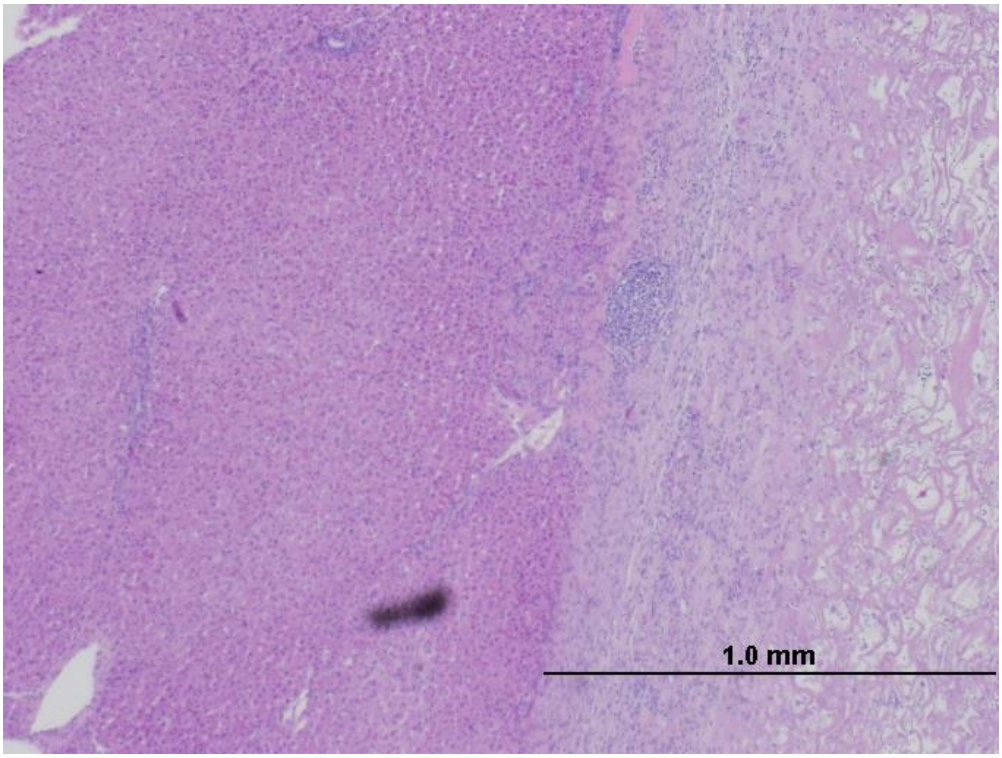

Figure 26: H&E staining of transplant interface after POD21 in study subject. Section was removed from the scaffold-liver interface in subject ADD7. It was observed that the scaffold (extreme right) was being absorbed into the fibrous tissue of the liver as part of the regenerative process. No signs of specific or significant reactions were detected. Observed using 4x objective lens.

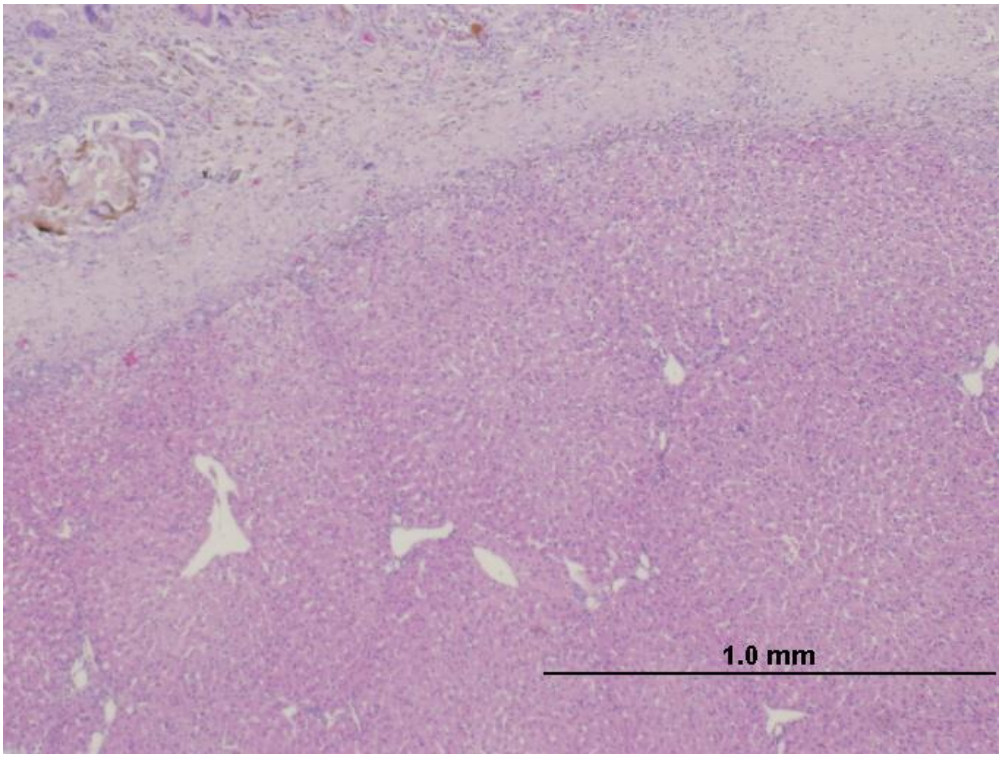

Figure 27: H&E stained lobules adjacent transplant interface of study subject. Section was removed from the scaffold-liver interface in subject ADD7. Healthy lobular structures were seen next to the regenerating fibrous tissue. No signs of fatty changes or cellular rejections were detected. Observed using 4x objective lens.

Peripheral Liver Histology

To investigate the overall condition of the liver, histological samples, located peripherally from the transplant interface were obtained and studied. Core tissue biopsy were performed on post-operative week 1 (see Figure 28) and week 2 (see Figure 29) to observe if any reactions were taking place due to the transplanted HLC. Week 3 samples (see Figure 30) were retrieved from the excised liver after euthanasia. Healthy lobular structures were seen and no signs of fatty changes or cellular rejections were detected, throughout the post-operative 3 weeks, in the peripheral locations. Figure 31 was obtained from the excised liver lobe after hepatectomy and used as a pre-op reference.

Figure 28: H&E stained liver biopsy on POD8 in study subject. Tissue was removed from subject ADD6's right liver lobe via core tissue biopsy. Healthy lobular structures are visible and no signs of fatty changes or cellular rejections were detected. Observed using 4x objective lens.

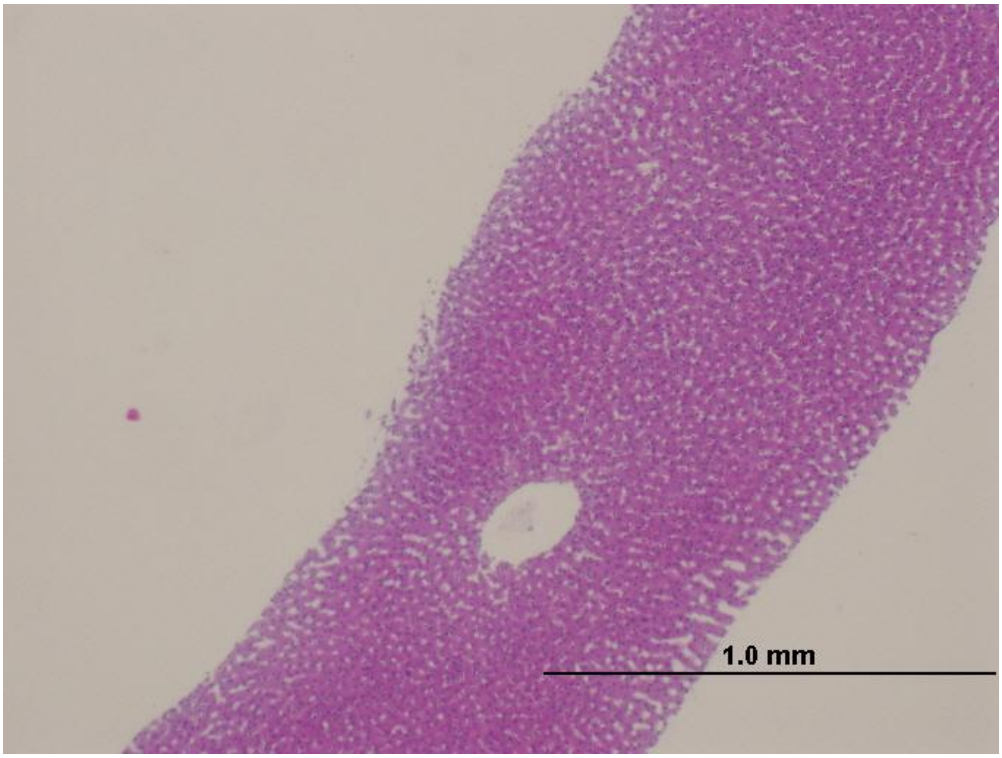

Figure 29: H&E stained liver biopsy on POD15 in study subject. Tissue was removed from subject ADD6's right liver lobe via core tissue biopsy. Healthy lobular structures are visible and no signs of fatty changes or cellular rejections were detected. Observed using 4x objective lens.

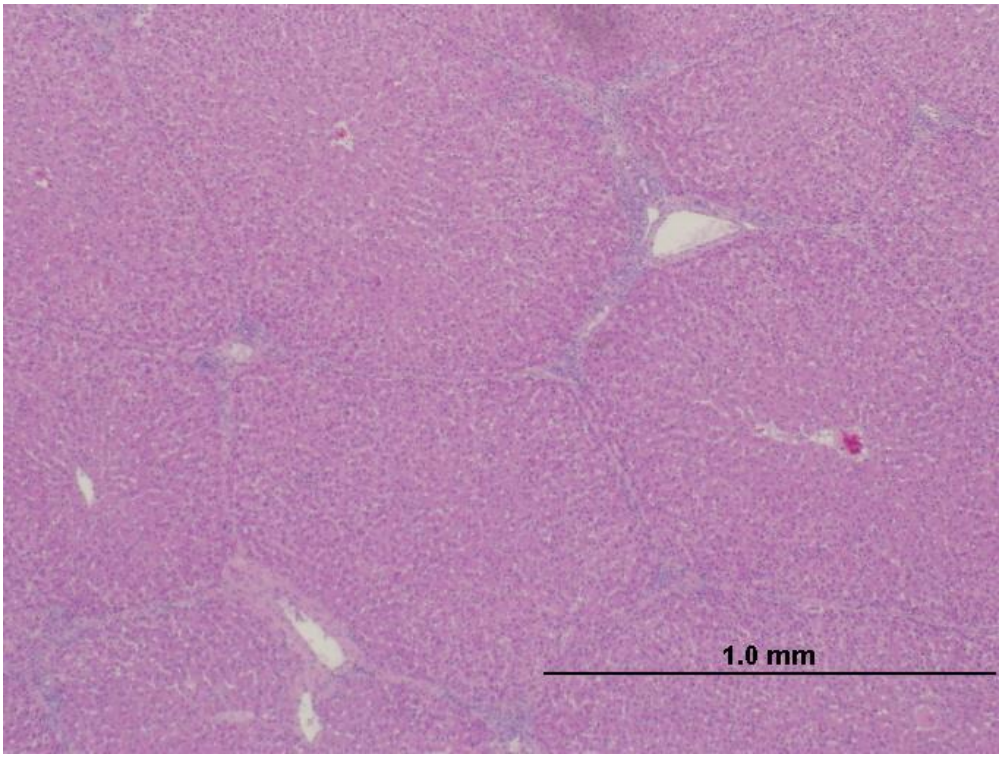

Figure 30: H&E stained liver sample on POD21 in study subject. Tissue was removed from subject ADD6's excised right liver lobe after euthanasia. Healthy lobular structures are visible and no signs of fatty changes or cellular rejections were detected. Observed using 4x objective lens.

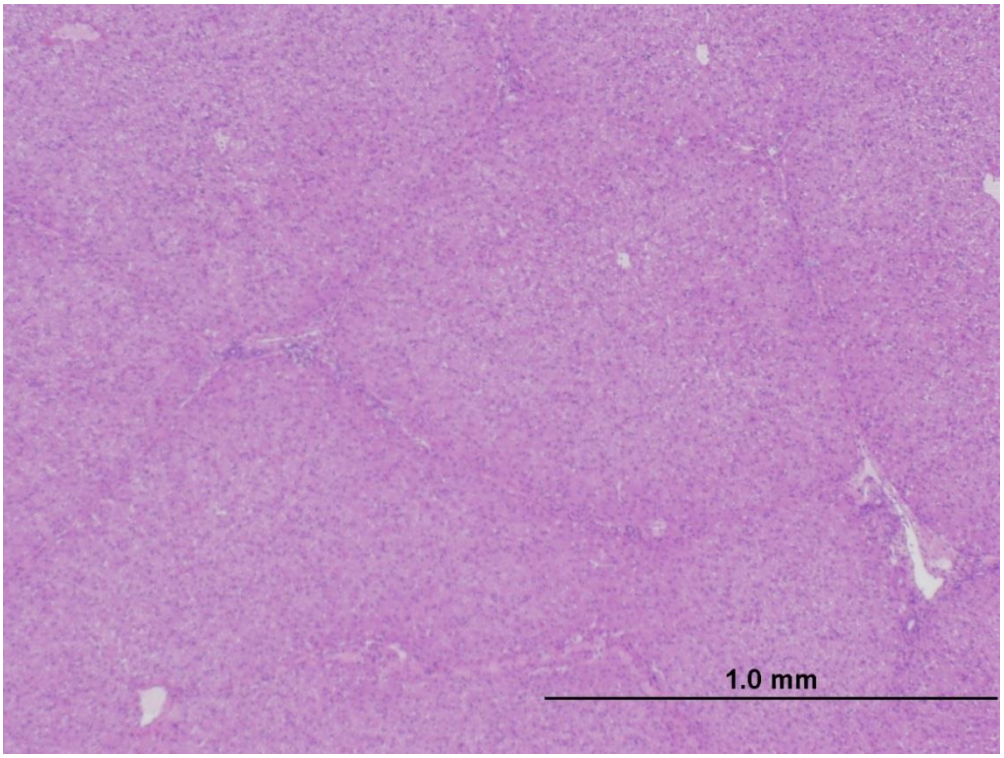

Figure 31: H&E stained pre-op liver sample from study subject. Tissue was removed from subject ADD6's excised left liver lobe after hepatectomy procedure. Post-operative histological samples' conditions were found comparable to that of pre-op sample, suggesting the insignificant toxicity of transplanted HLC. Observed using 4x objective lens.

Human Antigen Staining

From previous studies conducted, CLEC was found to possess immunosuppressive qualities and was able to survive in immunologically-competent hosts. Such characteristics for HLC, on the other hand, was still unclear. Staining for human antigens, allowed the team to check the viability of HLC 3 weeks after transplantation in a xeno-transplanted host. Bright field IHC was first performed on the scaffold with HLC for characterisation (see Figure 33). Human antigen staining was then carried out on paraffin sections from the study group. Analysis were compared with MT slides for scaffold localization. Figure 35 shows evidence of surviving HLC 3 weeks' post-transplantation. Figure 36 shows a porcine hepatic lobule from the same sample as negative control reference.

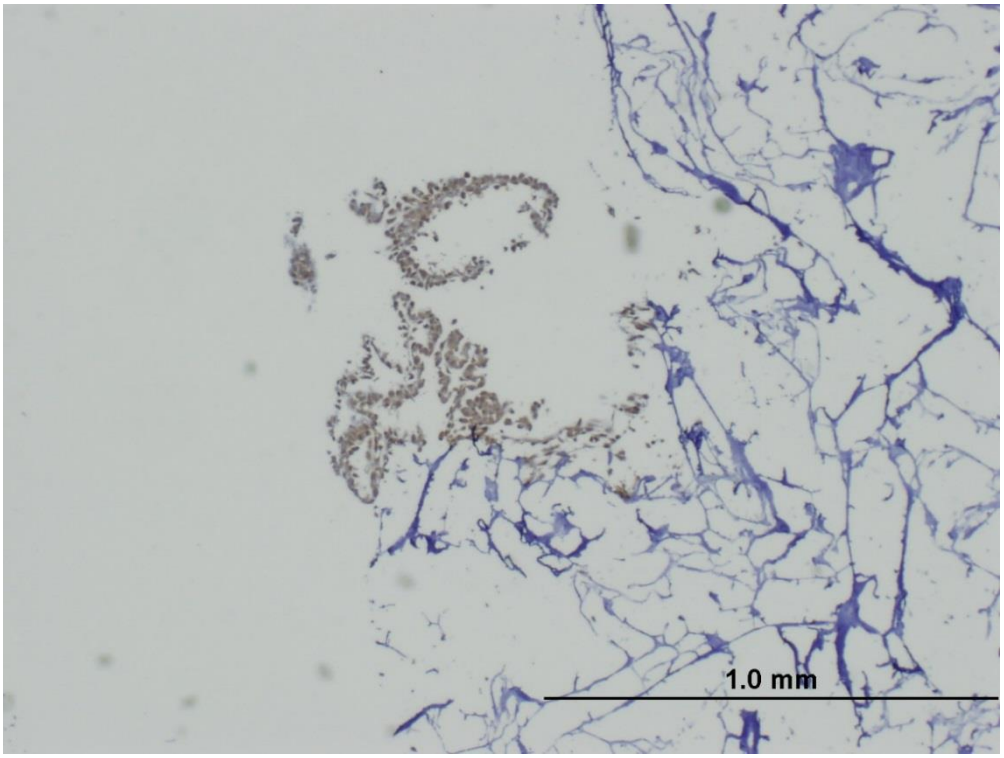

Figure 32: IHC staining of collagen scaffold with HLC. Scaffold was soaked in HLC for 5 minutes. HLC is clearly visible with its stained cytoplasm and nucleus. Observed using 4x objective lens.

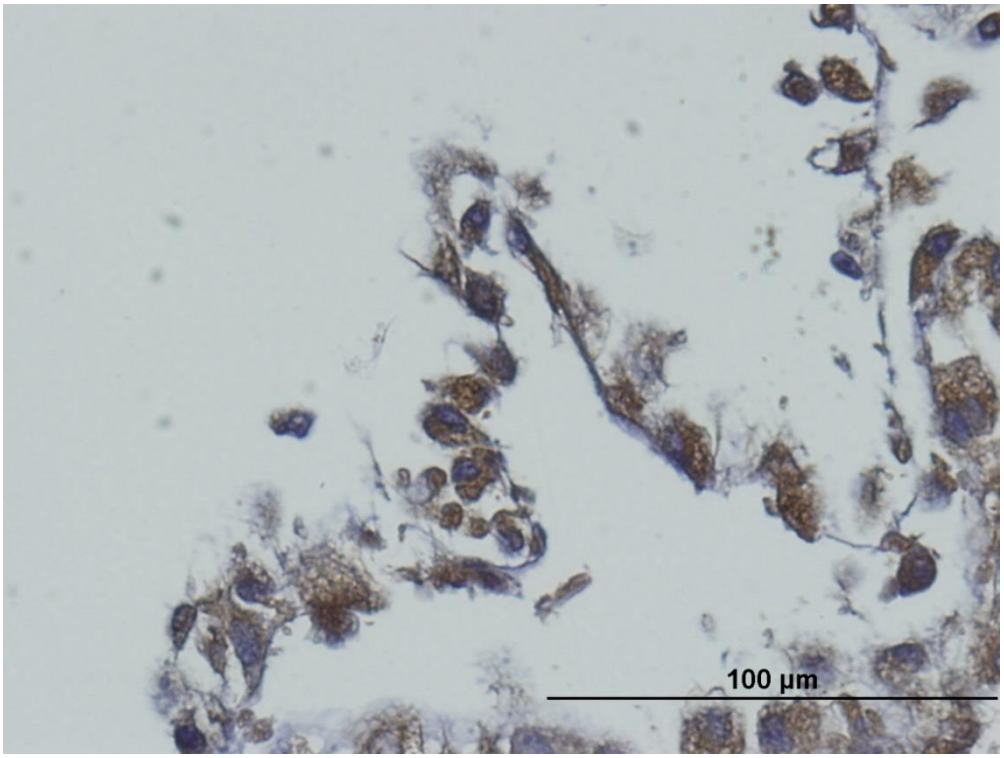

Figure 33: IHC staining of collagen scaffold with HLC (magnified). Scaffold was soaked in HLC for 5 minutes. HLC cytoplasm is stained dark with black nuclear staining. Observed using 40x objective lens.

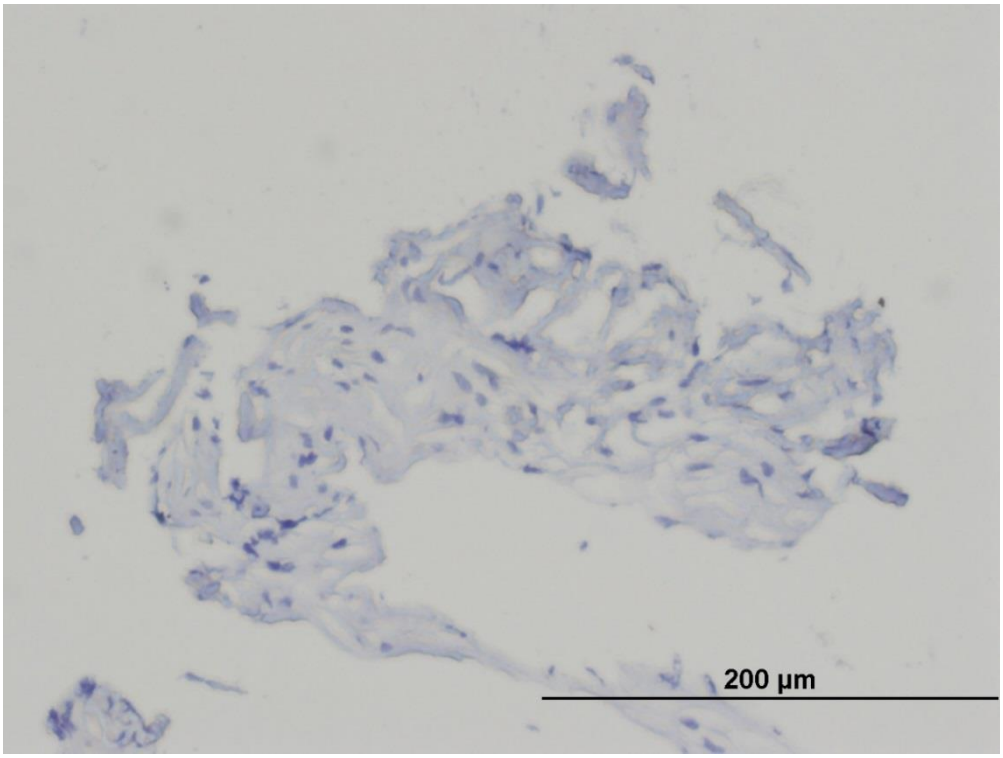

Figure 34: IHC staining of collagen scaffold after POD21 in study subject. Section was removed from subject ADD4 at same location as Figure 23. Dark cytoplasm is observed at collagen scaffold. Observed using 20x objective lens.

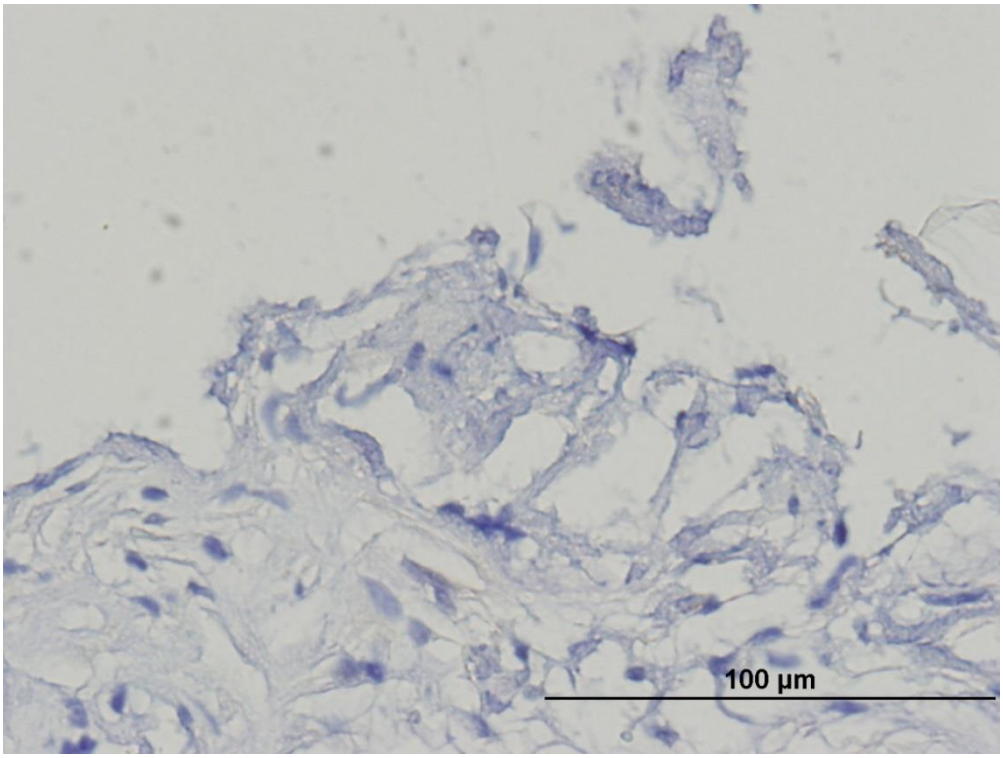

Figure 35: IHC staining of HLC after POD21 in study subject. Section was removed from subject ADD4 at same location as Figure 23. Dark cytoplasm is observed at collagen scaffold and black nuclear staining. Longitudinal cellular nuclear structure is comparable to that of Figure 33, suggesting evidence of HLC viability after 3 weeks' post transplantation. Observed using 40x objective lens.

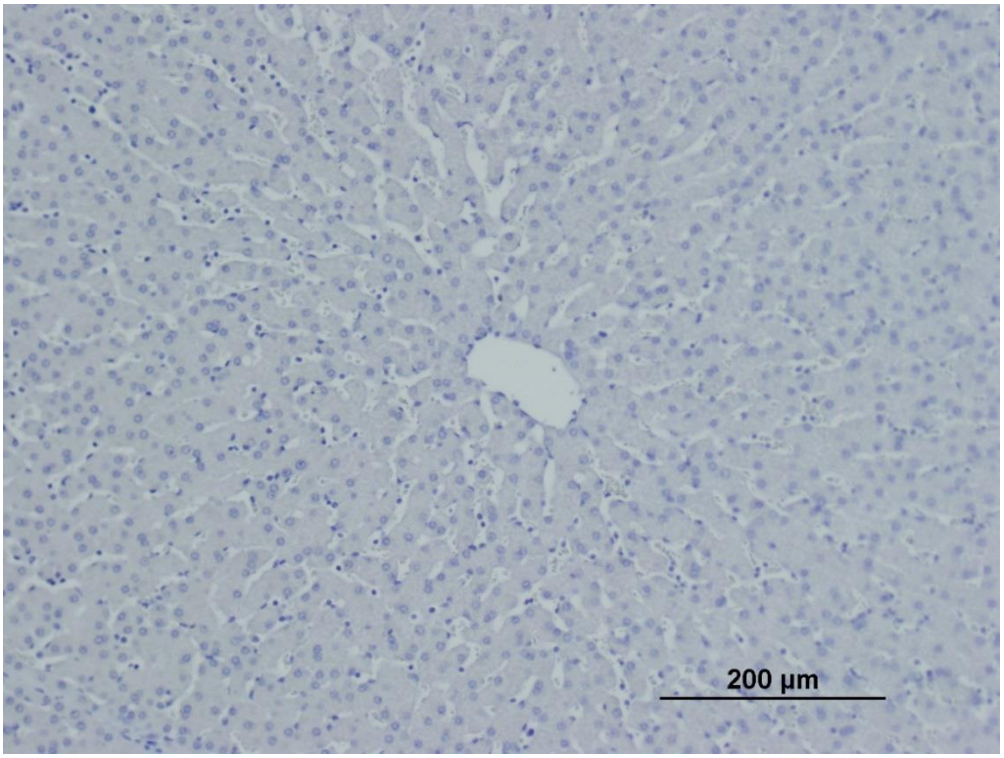

Figure 36: IHC staining of porcine lobule after POD21 in study subject. Section was removed from subject ADD4. Same paraffin section as Figure 34. Black nuclear staining is not detected. Observed using 10x objective lens.

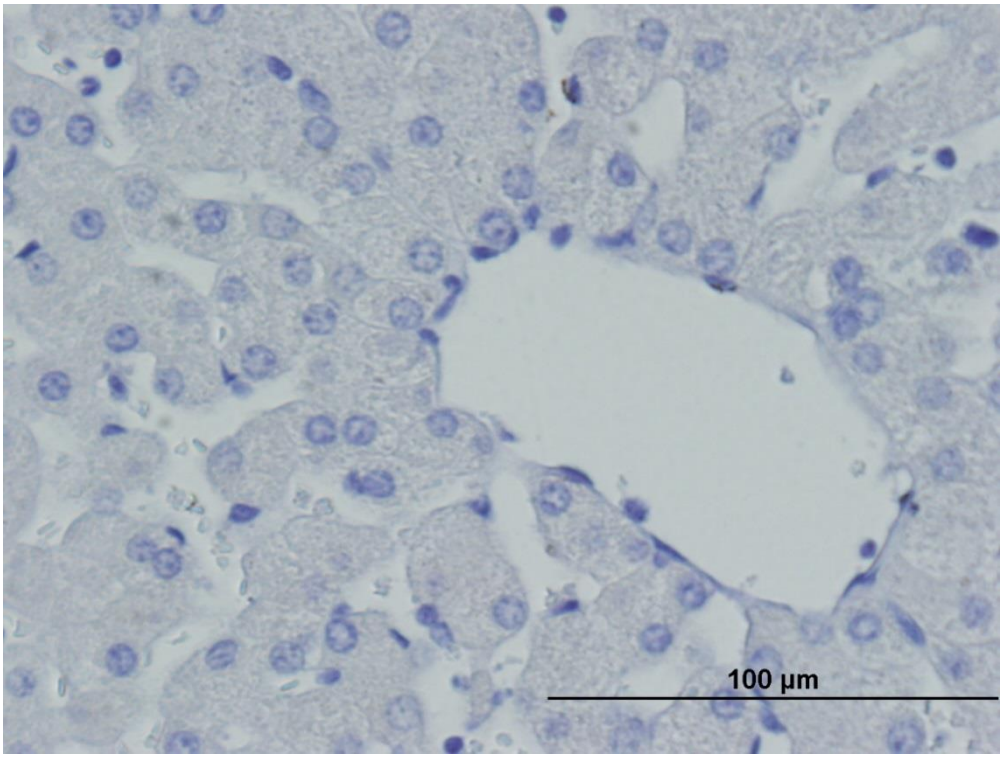

Figure 37: IHC staining of central vein after POD21 in study subject (magnified). Section was removed from subject ADD4. Same paraffin section as Figure 34. Black nuclear staining is not detected. Circular nuclear structure suggestive of porcine descent. Observed using 40x objective lens.

Discussion

Safety of Transplanted HLC

The first objective of this study was to evaluate the toxicity of transplanting HLC into a xeno-transplanted host. Starting from the LFT, no statistically significant differences were found between the control and study group in the aspects of cellular damage, synthetic function, biliary function and mass regeneration of the liver. All but one subject in the study group survived till post-operative 3 weeks, with intestinal adhesion as the likely early euthanasia reason. The transplant interfaces were evaluated and no signs of cellular rejections were observed for both groups. Healthy lobular structures were seen adjacent to the transplant interfaces. Histology performed on peripheral liver sites for post-operative week 1, week 2 and week 3 showed similar conditions as that of pre-transplantation of HLC.

However, few factors were not considered in this study which may have significant effects on the outcomes. Firstly, intraoperative blood loss during the 50% hepatectomy procedure was not considered. Clinical studies had shown that intraoperative blood loss has a negative impact on postoperative outcome for patients [63]. Similarly, the intraoperative blood loss for both groups may had been different, leading to a significant difference in the outcomes. Secondly, the percentage of surviving HLC after post-operative 3 weeks was not considered as well. Toxic effects may only be observed in significant amounts of HLC dosage, which may had been avoided after a percentage of HLC became unviable in the host liver. While the bright field IHC had shown evidence of viable HLC, the amount or spread of HLC could not be quantified. Florescent

microscopy, such as that of Figure 5, may had been a better method to quantify the amount of HLC present in the host liver.

Nevertheless, this study's findings do suggest the insignificant toxicity of transplanted HLC in a xeno-transplanted host. No statistical significant difference in the first few days were observed for the LFT, as the amount of viable HLC would had been the highest. Any cellular toxicity caused by HLC would also had been detected along the transplant interface due to local effects.

Collagen Scaffold Delivery Effectiveness

During the team's earlier research, different cell delivery methods were explored. HLC were transplanted intravenously into the liver, however, due to the "sticky" epithelial nature of HLC, the cells were found to accumulate in the hepatic portal venous system. This caused portal hypertension, leading to overall poor outcomes. Intraperitoneal infusion was also attempted. However, the HLC could not be localized to the liver, creating difficulties for further analysis on the cells.

This study had shown that using collagen scaffold, as a unique cell delivery vehicle, to be successful from the survival of HLC in xeno-transplanted host for 3 weeks' post-transplantation. However, the effectiveness of cell delivery was low. This is seen in Figure 20 where the inner layers of the collagen scaffold were not penetrated with HLC attaching to the collagen scaffold superficially. Collagen sandwich extra-cellular matrix, a system which has been well studied for the maintenance of mature hepatocyte function, is suggested for future works of HLC [64]. This too prevents the HLC from "escaping" to non-intended sites and mechanical injuries during surgical application.

Enhancement on Liver Regeneration

Despite not being able to detect any significant statistical difference in enhancement effects on liver regeneration for this small sample size study, a faster recovery trend seemed to be developing for the study arm. The study arm subjects may had suffered from a higher level of trauma during the hepatectomy, suggested by the higher DeRitis' Ratio in the first few days after the surgery. The ratio for the study arm dropped faster to reach the same level as that of the control arm in post-operative day 4. Certain ALP isoenzyme are clinically observed to be elevated which indicates for favourable liver regeneration. This may had been the case for the study arm during its recovery phase.

Nevertheless, several factors can be improved on to achieve the desired enhancement effect. Firstly, a significant amount of HLC may had "escaped" from the collagen scaffold during the initial period of transplantation. This is due to the superficial attachment of the HLC to the collagen scaffold observed. Furthermore, fibrous tissue was forming on the transplant interface, a part of the regenerative process of the host liver. This could have impeded any mitogenic effects HLC has on the host hepatocytes or assisting in the hepatocyte functions, in later periods of transplantation. This is where a multiple-layered sandwich collagen scaffold may be a solution to these problems. HLC will be confined in the scaffold and, similar to a delayed-release tablet, as the initial layers of collagen are being absorbed, HLC will continue to be exposed to host hepatocytes as the fibrous tissue degenerates during the later periods of the regeneration process.

Secondly, the injury caused to the host liver may had not been severe enough. Discussed above, proliferation of hepatocytes is the main mechanism of liver

repair and regeneration. Liver stem cells only come into play when there is insufficient hepatocyte proliferation activity. The porcine subjects used in this study were healthy and the strong organic hepatocyte regeneration may had overpowered any regenerative effects HLC had on the host liver. 50% hepatectomy procedure was the most severe surgical intervention the team could carried out due to survival risks on the subject. It is suggested that hepatotoxins, such as CCl_4, be administered in future studies to create a more severe liver insufficient model.

Thirdly, the HLC were not metabolically competent enough as compared to a mature hepatocyte. During the earlier study performed on *in-vitro* HLC, it was found that the metabolic enzyme expressions of HLC were approximately 70% lower compared to that of matured hepatocytes [60]. More work will have to be done to optimize the competency of HLC during the hepatogenesis stage. A benefit of using CLEC for cell therapy is the large number of viable cells obtained. With the insignificant toxicity levels of HLC, a large concentration of HLC could potentially be administered to offset the metabolic competency issue.

Conclusion

This study is the first step of the team's goal to use HLC, derived from CLEC, as a mean to enhance liver regeneration, before the liver worsens to a stage in which regeneration is not possible This study has shown the safety of transplanting HLC into an immunologically-competent xeno-transplanted host. It is also successful in showing the unique cell delivery method – applying collagen scaffold with HLC directly on the liver parenchyma surface – with the survival of the transported cells 3 weeks' post-transplantation. More investigations will have to be performed to show that HLC has a significant positive effect on liver regeneration. No doubt, this will be a long and arduous journey, but for patients suffering from liver diseases, this is a worthwhile effort.

List of References

1. Byass, P., *The global burden of liver disease: a challenge for methods and for public health.* BMC Med, 2014. **12**: p. 159.
2. Kim, W.R., et al., *OPTN/SRTR 2011 Annual Data Report: liver.* Am J Transplant, 2013. **13 Suppl 1**: p. 73-102.
3. Lopez-Terrada, D., et al., *Towards an international pediatric liver tumor consensus classification: proceedings of the Los Angeles COG liver tumors symposium.* Mod Pathol, 2014. **27**(3): p. 472-91.
4. Kuntz, E. and H.-D. Kuntz, *Morphology of the Liver*, in *Hepatology Textbook and Atlas*. 2008, Springer Berlin Heidelberg. p. 15-33.
5. Fasel, J.H.D., et al., *Macroscopic Anatomy of the Liver*, in *Textbook of Hepatology*. 2008, Blackwell Publishing Ltd. p. 1-8.
6. Court, F.G., et al., *Segmental nature of the porcine liver and its potential as a model for experimental partial hepatectomy.* Br J Surg, 2003. **90**(4): p. 440-4.
7. Frevert, U., et al., *Intravital Observation of Plasmodium berghei Sporozoite Infection of the Liver.* PLoS Biol, 2005. **3**(6): p. e192.
8. Bioulac-Sage, P., B. Le Bail, and C. Balabaud, *Liver and Biliary Tract Histology*, in *Textbook of Hepatology*. 2008, Blackwell Publishing Ltd. p. 9-19.
9. Kuntz, E. and H.-D. Kuntz, *Biochemistry and Functions of the Liver*, in *Hepatology Textbook and Atlas*. 2008, Springer Berlin Heidelberg. p. 35-76.
10. Renato, P., et al., *Functions of the Liver*, in *Textbook of Hepatology*. 2008, Blackwell Publishing Ltd. p. 89-128.
11. Rigato, I., J.D. Ostrow, and C. Tiribelli, *Biochemical Investigations in the Management of Liver Disease*, in *Textbook of Hepatology*. 2008, Blackwell Publishing Ltd. p. 451-467.
12. Kuntz, E. and H.-D. Kuntz, *Laboratory diagnostics*, in *Hepatology Textbook and Atlas*. 2008, Springer Berlin Heidelberg. p. 95-130.
13. Bolondi, L., et al., *Imaging of the Liver*, in *Textbook of Hepatology*. 2008, Blackwell Publishing Ltd. p. 500-548.
14. Niehues, S.M., et al., *Liver volume measurement: reason of the difference between in vivo CT-volumetry and intraoperative ex vivo determination and how to cope it.* Eur J Med Res, 2010. **15**(8): p. 345-50.
15. Zhou, J., et al., *Longitudinal in-vivo volumetry study for porcine liver regeneration from CT data.* Conf Proc IEEE Eng Med Biol Soc, 2014. **2014**: p. 4743-6.
16. *Radiological diagnostics*, in *Hepatology Textbook and Atlas: History • Morphology Biochemistry • Diagnostics Clinic • Therapy*. 2008, Springer Berlin Heidelberg: Berlin, Heidelberg. p. 177-198.
17. Thavarajah, R., et al., *Chemical and physical basics of routine formaldehyde fixation.* Journal of Oral and Maxillofacial Pathology : JOMFP, 2012. **16**(3): p. 400-405.
18. Mireskandari, M. and I. Petersen, *Clinical Pathology*, in *Ex-vivo and In-vivo Optical Molecular Pathology*. 2014, Wiley-VCH Verlag GmbH & Co. KGaA. p. 1-26.
19. Desmet, V.J., T. Roskams, and M. Bruguera, *Histological Features*, in *Textbook of Hepatology*. 2008, Blackwell Publishing Ltd. p. 421-432.
20. Krishna, M., *Role of special stains in diagnostic liver pathology.* Clinical Liver Disease, 2013. **2**(S1): p. S8-S10.
21. Malek, N.P., K.L. Rudolph, and A.M. Diehl, *Regulation of the Liver Cell Mass*, in *Textbook of Hepatology*. 2008, Blackwell Publishing Ltd. p. 274-289.

22. Kuntz, E. and H.-D. Kuntz, *Clinical and morphological principles*, in *Hepatology Textbook and Atlas*. 2008, Springer Berlin Heidelberg. p. 397-417.
23. Roskams, T., *Hepatic Stem Cells*, in *Textbook of Hepatology*. 2008, Blackwell Publishing Ltd. p. 58-64.
24. Fausto, N., *Liver regeneration and repair: hepatocytes, progenitor cells, and stem cells.* Hepatology, 2004. **39**(6): p. 1477-87.
25. Huch, M., *Regenerative biology: The versatile and plastic liver.* Nature, 2015. **517**(7533): p. 155-156.
26. Lowes, K.N., et al., *Oval Cell Numbers in Human Chronic Liver Diseases Are Directly Related to Disease Severity.* The American Journal of Pathology, 1999. **154**(2): p. 537-541.
27. Tani, M., et al., *Regulating factors of liver regeneration after hepatectomy.* Cancer Chemother Pharmacol, 1994. **33 Suppl**: p. S29-32.
28. Huh, C.G., et al., *Hepatocyte growth factor/c-met signaling pathway is required for efficient liver regeneration and repair.* Proc Natl Acad Sci U S A, 2004. **101**(13): p. 4477-82.
29. Michalopoulos, G.K., *Liver regeneration.* J Cell Physiol, 2007. **213**(2): p. 286-300.
30. Michalopoulos, G.K., *Liver regeneration after partial hepatectomy: critical analysis of mechanistic dilemmas.* Am J Pathol, 2010. **176**(1): p. 2-13.
31. Taub, R., *Liver regeneration: from myth to mechanism.* Nat Rev Mol Cell Biol, 2004. **5**(10): p. 836-47.
32. Christodoulidou, A., et al., *The Roles of Telomerase in the Generation of Polyploidy during Neoplastic Cell Growth.* Neoplasia (New York, N.Y.), 2013. **15**(2): p. 156-168.
33. Celton-Morizur, S. and C. Desdouets, *Polyploidization of liver cells*, in *Polyploidization and Cancer*, R.Y.C. Poon, Editor. 2010, Springer New York: New York, NY. p. 123-135.
34. Miyaoka, Y. and A. Miyajima, *To divide or not to divide: revisiting liver regeneration.* Cell Division, 2013. **8**: p. 8-8.
35. M., B.L., et al., *The Role of Hepatocyte Enlargement in Hepatic Pressure in Cirrhotic and Noncirrhotic Alcoholic Liver Disease.* Hepatology, 1982. **2**(5): p. 539S--546S.
36. Moreira, R.K., *Hepatic stellate cells and liver fibrosis.* Arch Pathol Lab Med, 2007. **131**(11): p. 1728-34.
37. Yin, C., et al., *Hepatic stellate cells in liver development, regeneration, and cancer.* J Clin Invest, 2013. **123**(5): p. 1902-10.
38. Friedman, S.L., *Cellular and Molecular Pathobiology of Liver Fibrosis and its Pharmacological Intervention.* 2008: p. 590--603.
39. Kuntz, E. and H.-D. Kuntz, *Liver cirrhosis*, in *Hepatology Textbook and Atlas*. 2008, Springer Berlin Heidelberg. p. 737-772.
40. Kuntz, E. and H.-D. Kuntz, *Chronic hepatitis*, in *Hepatology Textbook and Atlas*. 2008, Springer Berlin Heidelberg. p. 711-736.
41. Friedman, S.L., *Liver fibrosis – from bench to bedside.* Journal of Hepatology, 2003. **38**: p. 38-53.
42. Iredale, J.P. and G.I. Neil, *The Evolution of Cirrhosis.* 2008: p. 581--589.
43. Guha, I.N. and I.J. P., *Clinical and Diagnostic Aspects of Cirrhosis.* 2008: p. 604--619.
44. Kuntz, E. and H.-D. Kuntz, *Treatment of liver diseases*, in *Hepatology Textbook and Atlas*. 2008, Springer Berlin Heidelberg. p. 871-922.
45. Guyader, D., *The General Management of Liver Diseases*, in *Textbook of Hepatology*. 2008, Blackwell Publishing Ltd. p. 1897-1904.

46. Everson, G.T. and F.E. Membreno, *Liver Transplantation: Indications, Contraindications and Results*, in *Textbook of Hepatology*. 2008, Blackwell Publishing Ltd. p. 1984-1995.
47. Neuberger, J., *Immunosuppression*, in *Textbook of Hepatology*. 2008, Blackwell Publishing Ltd. p. 2003-2009.
48. Alison, M.R., S. Islam, and S. Lim, *Stem cells in liver regeneration, fibrosis and cancer: the good, the bad and the ugly.* J Pathol, 2009. **217**(2): p. 282-98.
49. Kuntz, E. and H.-D. Kuntz, *Acute and chronic liver insufficiency*, in *Hepatology Textbook and Atlas*. 2008, Springer Berlin Heidelberg. p. 379-396.
50. Dhawan, A., et al., *Human hepatocyte transplantation: current experience and future challenges.* Nat Rev Gastroenterol Hepatol, 2010. **7**(5): p. 288-298.
51. Abdel Aziz, M.T., et al., *Therapeutic potential of bone marrow-derived mesenchymal stem cells on experimental liver fibrosis.* Clin Biochem, 2007. **40**(12): p. 893-9.
52. Tsai, P.C., et al., *The therapeutic potential of human umbilical mesenchymal stem cells from Wharton's jelly in the treatment of rat liver fibrosis.* Liver Transpl, 2009. **15**(5): p. 484-95.
53. Siddiqui, A., J. T, and N. Anusha P, *Stem Cell Therapy for Liver Diseases.* Journal of Stem Cell Research & Therapy, 2011. **01**(03).
54. Wells, R.G., *The epithelial-to-mesenchymal transition in liver fibrosis: here today, gone tomorrow?* Hepatology, 2010. **51**(3): p. 737-40.
55. Lim, I.J. and T.T. Phan, *Epithelial and mesenchymal stem cells from the umbilical cord lining membrane.* Cell Transplant, 2014. **23**(4-5): p. 497-503.
56. Ruetze, M., et al., *Common features of umbilical cord epithelial cells and epidermal keratinocytes.* J Dermatol Sci, 2008. **50**(3): p. 227-31.
57. Zhou, Y., et al., *Characterization of human umbilical cord lining-derived epithelial cells and transplantation potential.* Cell Transplant, 2011. **20**(11-12): p. 1827-41.
58. Reza, H.M., et al., *Umbilical cord lining stem cells as a novel and promising source for ocular surface regeneration.* Stem Cell Rev, 2011. **7**(4): p. 935-47.
59. Sivalingam, J., et al., *Biosafety assessment of site-directed transgene integration in human umbilical cord-lining cells.* Mol Ther, 2010. **18**(7): p. 1346-56.
60. Cheong, H.H., et al., *Metabolically functional hepatocyte-like cells from human umbilical cord lining epithelial cells.* Assay Drug Dev Technol, 2013. **11**(2): p. 130-8.
61. Hoffmaster, K.A., et al., *P-glycoprotein Expression, Localization, and Function in Sandwich-Cultured Primary Rat and Human Hepatocytes: Relevance to the Hepatobiliary Disposition of a Model Opioid Peptide.* Pharmaceutical Research, 2004. **21**(7): p. 1294-1302.
62. Dunn, J.C.Y.a.T.R.G.a.Y.M.L., *Long-Term in Vitro Function of Adult Hepatocytes in a Collagen Sandwich Configuration.* Biotechnology Progress, 1991. **7**(3): p. 237--245.
63. Alkozai, E.M., T. Lisman, and R.J. Porte, *Bleeding in liver surgery: prevention and treatment.* Clin Liver Dis, 2009. **13**(1): p. 145-54.
64. Dunn, J.C., et al., *Hepatocyte function and extracellular matrix geometry: long-term culture in a sandwich configuration.* Faseb j, 1989. **3**(2): p. 174-7.

Appendix A

Immunohistochemistry Protocol for Paraffin sections

1. Deparaffinize sections: 2 changes of xylene, 10 minutes each
2. Rehydrate: 2 changes of absolute alcohol, 5 minutes each, 95% alcohol for 2 minutes and 70% alcohol for 2 minutes.
3. Antigen expose epitope using citrate buffer (pH 6.1) at 121 °C for 40 minutes.
4. Block endogenous peroxides: 15 minutes at room temperature in 3% H_2O_2 in PBS.
5. 10% Goat serum in PBS-T, block for 30 minutes.
6. 1^{st} Antibody: Dilute 1^{st} Ab in antibody diluents, apply 50ul/section. Incubate overnight at 4 °C in humid chamber.
7. Wash slides in gentle running tap water for 10 minutes.
8. Rinse in PBS-T for 5 minutes.
9. 2^{nd} Antibody: Dilute 2^{nd} Ab in antibody diluents, apply 50ul/section. Incubate for 30 minutes at room temperature in humid chamber.
10. Wash slides in gentle running tap water for 10 minutes.
11. Rinse in PBS-T for 5 minutes.
12. Incubate sections in DAB for 5 minutes.
13. Drain and rinse under deionized water to stop DAB reaction.
14. Counter stain with hematoxylin: 10 quick dips in hematoxylin, Rinse with dH_2O, Develop in tap water for 5 minutes, Dip 5 times in acid ethanol, Rinse in tap water for 2 minutes, Rinse with dH_2O for 2 minutes.
15. Dehydrate through 95% alcohol, 2 changes of absolute alcohol, 5 minutes each.
16. Clear in 2 changes of xylene, 5 minutes each.
17. Mount with xylene based medium.

Appendix B

Table 2: Raw LFT data of subject CARE9 from control group.

CARE9									
Result	Post-Op 08-May-13	POD 1 09-May-13	POD 2 10-May-13	POD 4 12-May-13	POD 6 14-May-13	POD 8 16-May-13	POD 15 23-May-13	POD21 29-May-13	UNITS
PT	13.1	14.7	13.7	11.9	12.8	13.2	*	12.9	secs
INR	1.04	1.21	1.11	0.92	1.01	1.05	*	1.02	INR
ALB	26	29	27	30	33	38	32	30	g/L
TBIL	2	15	6	3	2	2	2	2	umol/L
DB	1	10	5	2	1	1	1	2	umol/L
IB	1	5	1	1	1	1	1	0	umol/L
AST	28	670	212	60	39	86	91	35	U/L
ALT	51	113	95	90	73	89	79	62	U/L
ALP	123	224	223	178	153	142	130	98	U/L
LDH	902	2682	1757	1613	1268	1664	1824	988	U/L

* – Lack of data due to technical difficulties (e.g. clotted blood tubes, dysfunctional portal catheter)

Table 3: Raw LFT data of subject CARE12 from control group.

CARE12									
Result	Post-Op 12-Jun-13	POD1 13-Jun-13	POD2 14-Jun-13	POD4 16-Jun-13	POD6 18-Jun-13	POD8 22-Jun-13	POD15 29-Jun-13	POD21 3-Jul-13	UNITS
PT	13.6	15.2	13.3	12.8	12.4	13.3	14	*	secs
INR	1.09	1.27	1.06	1.01	0.97	1.06	1.14	*	INR
ALB	21	29	30	30	31	31	31	26	g/L
TBIL	2	14	2	2	2	2	2	2	umol/L
DB	1	11	2	1	2	1	1	2	umol/L
IB	1	3	0	1	0	1	1	0	umol/L
AST	51	747	334	113	72	46	63	68	U/L
ALT	41	106	109	104	93	80	70	43	U/L
ALP	94	250	210	125	100	77	90	106	U/L
LDH	1321	2914	2321	2358	1919	1410	1368	1144	U/L

* – Lack of data due to technical difficulties (e.g. clotted blood tubes, dysfunctional portal catheter)

Table 4: Raw LFT data of subject ADD2 from control group.

ADD2									
Result	Post-Op 22-Jul-15	POD1 23-Jul-15	POD2 24-Jul-15	POD4 26-Jul-15	POD6 28-Jul-15	POD8 30-Jul-15	POD15 6-Aug-15	POD21 12-Aug-15	UNITS
PT	14.8	14.6	13.1	12.8	14.1	12.7	12.5	*	secs
INR	1.20	1.18	1.03	1.00	1.13	0.99	0.97	*	INR
ALB	15	23	24	25	28	27	25	*	g/L
TBIL	2	15	3	3	3	2	3	*	umol/L
DB	1	5	1	1	1	1	1	*	umol/L
IB	1	10	2	2	2	1	2	*	umol/L
AST	111	292	135	52	56	39	54	*	U/L
ALT	50	105	114	98	100	76	50	*	U/L
ALP	117	276	251	281	462	305	122	*	U/L
LDH	904	2217	2190	1681	1748	1533	1647	*	U/L

* – Lack of data due to technical difficulties (e.g. clotted blood tubes, dysfunctional portal catheter)

Table 5: Raw LFT data of subject ADD3 from control group.

ADD3									
Result	Post-Op	POD1	POD2	POD4	POD6	POD8	POD15	POD21	UNITS
	12-Aug-15	13-Aug-15	14-Aug-15	16-Aug-15	18-Aug-15	20-Aug-15	27-Aug-15	N/A	
PT	*	13.5	12.4	13.4	13.0	11.9	13.3	N/A	**secs**
INR	*	1.07	0.96	1.06	1.02	0.91	1.05	N/A	**INR**
ALB	19	29	26	26	20	15	N/A	N/A	**g/L**
TBIL	2	11	4	3	7	5	N/A	N/A	**umol/L**
DB	1	3	1	1	2	1	N/A	N/A	**umol/L**
IB	1	8	3	2	5	4	N/A	N/A	**umol/L**
AST	227	565	200	52	172	74	N/A	N/A	**U/L**
ALT	59	116	113	95	67	41	N/A	N/A	**U/L**
ALP	127	301	256	177	199	89	N/A	N/A	**U/L**
LDH	1335	4689	2503	1913	1923	1370	N/A	N/A	**U/L**

* – Lack of data due to technical difficulties. N/A – Subject was euthanized before testing

Table 6: Raw LFT data of subject CARE10 from study group.

CARE10									
Result	Post-Op	POD1	POD2	POD4	POD6	POD8	POD15	POD21	UNITS
	15-May-13	16-May-13	17-May-13	19-May-13	21-May-13	23-May-13	30-May-13	5-Jun-13	
PT	12.5	14.7	13.4	13.3	12.8	12.3	13.3	*	**secs**
INR	0.98	1.21	1.07	1.06	1.01	0.96	1.06	*	**INR**
ALB	30	32	32	29	28	33	31	*	**g/L**
TBIL	2	5	6	5	2	2	2	*	**umol/L**
DB	1	4	4	3	2	1	1	*	**umol/L**
IB	1	1	2	2	0	1	1	*	**umol/L**
AST	227	2641	1038	202	82	128	133	*	**U/L**
ALT	63	164	159	112	92	97	81	*	**U/L**
ALP	93	276	331	267	195	130	100	*	**U/L**
LDH	994	9057	3262	2101	1434	1650	1445	*	**U/L**

* – Lack of data due to technical difficulties (e.g. clotted blood tubes, dysfunctional portal catheter)

Table 7: Raw LFT data of subject CARE11 from study group.

CARE11									
Result	Post-Op	POD1	POD2	POD4	POD6	POD8	POD15	POD21	UNITS
	22-May-13	23-May-13	24-May-13	26-May-13	28-May-13	30-May-13	6-Jun-13	12-Jun-13	
PT	12.4	14	*	11.9	12.8	13.2	*	*	**secs**
INR	0.97	1.14	*	0.92	1.01	1.05	*	*	**INR**
ALB	23	26	29	30	33	38	*	*	**g/L**
TBIL	2	12	3	3	2	2	*	*	**umol/L**
DB	1	8	2	2	1	1	*	*	**umol/L**
IB	1	4	1	1	1	1	*	*	**umol/L**
AST	27	811	306	60	39	86	*	*	**U/L**
ALT	60	192	212	90	73	89	*	*	**U/L**
ALP	102	192	187	178	153	142	*	*	**U/L**
LDH	981	5491	3111	1613	1268	1664	*	*	**U/L**

* – Lack of data due to technical difficulties (e.g. clotted blood tubes, dysfunctional portal catheter)

Table 8: Raw LFT data of subject CARE14 from study group.

CARE14									
Result	Post-Op	POD1	POD2	POD4	POD6	POD8	POD15	POD21	UNITS
	21-Jun-13	22-Jun-13	23-Jun-13	25-Jun-13	27-Jun-13	29-Jun-13	6-Jul-13	N/A	
PT	12.1	13.9	13.9	13	12.6	13.1	13.3	N/A	**secs**
INR	0.94	1.13	1.13	1.03	0.99	1.04	1.06	N/A	**INR**
ALB	28	31	30	24	25	28	16	N/A	**g/L**
TBIL	2	21	12	10	13	6	2	N/A	**umol/L**
DB	1	13	9	8	10	5	2	N/A	**umol/L**
IB	1	8	3	2	3	1	0	N/A	**umol/L**
AST	148	2073	864	163	85	51	138	N/A	**U/L**
ALT	60	170	132	78	60	68	68	N/A	**U/L**
ALP	89	375	312	227	207	182	86	N/A	**U/L**
LDH	1160	11000	3859	1885	1622	1459	1852	N/A	**U/L**

N/A – Subject was euthanized before testing

Table 9: Raw LFT data of subject ADD4 from study group.

ADD4									
Result	Post-Op 19-Aug-15	POD1 20-Aug-15	POD2 21-Aug-15	POD4 23-Aug-15	POD6 25-Aug-15	POD8 27-Aug-15	POD15 3-Sep-15	POD21 9-Sep-15	UNITS
PT	13.1	13.6	12.9	12.2	11.9	12.7	13.1	11.8	secs
INR	1.03	1.08	1.01	0.94	0.91	0.99	1.03	0.90	INR
ALB	20	31	30	30	32	26	21	30	g/L
TBIL	3	12	9	3	4	3	4	3	umol/L
DB	1	4	3	1	1	1	1	1	umol/L
IB	2	8	6	2	3	2	3	2	umol/L
AST	137	556	178	59	46	30	27	27	U/L
ALT	60	129	140	124	105	66	50	77	U/L
ALP	163	395	314	269	232	153	106	123	U/L
LDH	1553	4437	2300	1819	1884	1116	883	951	U/L

Table 10: Raw LFT data of subject ADD6 from study group.

ADD6									
Result	Post-Op 21-Oct-15	POD1 22-Oct-15	POD2 23-Oct-15	POD4 25-Oct-15	POD6 27-Oct-15	POD8 29-Oct-15	POD15 5-Nov-15	POD21 11-Nov-15	UNITS
PT	17.8	14.7	12.8	13.2	12.5	13.2	13.0	13.0	secs
INR	1.52	1.19	1.00	1.05	0.98	1.05	1.03	1.03	INR
ALB	15	25	27	27	33	26	27	31	g/L
TBIL	2	11	3	3	3	4	4	4	umol/L
DB	1	4	1	1	3	1	1	1	umol/L
IB	1	7	2	2	0	3	3	3	umol/L
AST	139	2202	876	118	70	53	34	43	U/L
ALT	35	181	226	173	165	103	71	80	U/L
ALP	77	239	198	123	120	92	66	74	U/L
LDH	863	13751	5633	3287	3247	2001	1241	1232	U/L

Table 11: Raw LFT data of subject ADD7 from study group.

ADD7									
Result	Post-Op 3-Nov-15	POD1 04-Nov-15	POD2 5-Nov-15	POD4 7-Nov-15	POD6 9-Nov-15	POD8 11-Nov-15	POD15 18-Nov-15	POD21 24-Nov-15	UNITS
PT	15.4	15.0	13.4	13.4	13.4	13.3	13.2	12.7	secs
INR	1.27	1.23	1.07	1.07	1.07	1.06	1.05	1.00	INR
ALB	19	32	30	33	29	25	27	32	g/L
TBIL	2	10	4	4	3	4	3	3	umol/L
DB	1	3	1	1	1	1	1	1	umol/L
IB	1	7	3	3	2	3	2	2	umol/L
AST	161	1072	455	97	42	57	32	37	U/L
ALT	51	176	181	167	106	87	79	84	U/L
ALP	93	248	211	126	90	99	139	150	U/L
LDH	1115	9757	3260	2386	1643	1477	1300	1408	U/L

Table 12: Raw LFT data of subject ADD9 from study group.

ADD9									
Result	Post-Op 04-Feb-16	POD1 05-Feb-16	POD2 07-Feb-16	POD4 09-Feb-16	POD6 11-Feb-16	POD8 18-Feb-16	POD15 24-Feb-16	POD21 25-Feb-16	UNITS
PT	12.9	15	13.5	*	*	13.5	13.8	13.1	secs
INR	1.02	1.23	1.08	*	*	1.08	1.11	1.04	INR
ALB	18	28	29	*	*	23	22	27	g/L
TBIL	3	9	3	*	*	3	3	5	umol/L
DB	1	3	1	*	*	1	1	1	umol/L
IB	2	6	2	*	*	2	2	4	umol/L
AST	104	773	314	*	*	30	41	28	U/L
ALT	49	142	157	*	*	69	52	65	U/L
ALP	115	241	229	*	*	94	99	92	U/L
LDH	1214	4247	2258	*	*	1041	936	948	U/L

* – Lack of data due to technical difficulties (e.g. clotted blood tubes, dysfunctional portal catheter)

Appendix C

Table 13: Raw liver volume data of porcine subjects.

Liver Volume (*ml*)					
Result	**Pre-Op**	**Post-Op**	**POD8**	**POD15**	**POD21***
CONTROL					
CARE9	1226.8	522.8	940.5	1109.3	1000
CARE12	1044.5	498.2	876.3	904.1	1100
ADD2	719	550	684	826	711.9
ADD3	835	471	760	496	N/A
STUDY					
CARE10	1223	489.8	974.2	1117	1100
CARE11	1459.5	801.4	1166.2	1267.3	1200
CARE14	1156.3	296.2	701	643.3	N/A
ADD4	839	688	783	867	711.9
ADD6	787	573	884	863	762.75
ADD7	730	594	804	724	734.5
ADD9	684	397	651	740	576.3

N/A – Subject was euthanized before testing.
* – Additional 13% volume was accounted for water displacement method.